LIMNOLOGY
AND
OCEANOGRAPHY

December 1996
Volume 41
Number 8

Limnol. Oceanogr., 41(8), 1996, 1591–1609

Modeling bacterial utilization of dissolved organic matter: Optimization replaces Monod growth kinetics

J. J. Vallino, C. S. Hopkinson, and J. E. Hobbie
Ecosystems Center, Marine Biological Laboratory, Woods Hole, Massachusetts 02543

Abstract

A bioenergetic model has been developed to examine growth kinetics associated with bacterial utilization of dissolved organic matter (DOM), NH_4^+, and NO_3^-. A set of 11 metabolic reactions are used to govern the incorporation, oxidation, and N remineralization of DOM and dissolved inorganic N associated with bacterial growth. For each reaction, free energies and electron transfer requirements are calculated based on the C, H, O, and N composition of the substrates and their concentration in the environment. From these reactions, an optimization problem is constructed in which bacterial growth rate is maximized subject to constraints on energetics, electron balances, substrate uptake kinetics, and bacterial C:N ratio. The optimization approach provides more information on bacterial growth kinetics than do the Monod-type models that are typically used to describe bacterial growth. Simulations are run to examine bacterial C yield and growth rate, N remineralization or immobilization, and substrate preferences as resource concentrations and compositions are varied. Results from the model agree well with observations in the literature, which indicate that the premise of the model, that bacteria allocate resources to maximize growth rate, may be an accurate overall description of bacterial growth. Simulations indicate that bacterial growth rate and yield are strongly correlated to the oxidation state of the labile DOM, as determined from its bulk elemental composition. Furthermore, the model demonstrates that bacterial growth cannot always be explained by a single constraint (such as the C:N ratio of substrate), since several constraints are often active simultaneously and continuously change with environmental conditions.

Dissolved organic matter (DOM) represents an important component of aquatic ecosystems in terms of both the size of the compartment relative to particulate organic matter (POM) and its impact on the functioning of microbial food webs. Consequently, many descriptive and experimental studies have been conducted to characterize the composition of DOM, examine its production and utilization, understand its impact on microbial dynamics, and determine the extent to which it supports higher trophic levels. The results of these studies have been incorporated to various extents in both simple bacterial growth models and more complete food web models that examine DOM utilization. These models are based almost exclusively on Monod-type growth expressions in which bacterial C yield (mol bacterial C/mol C consumed, also called bacterial growth efficiency) and maximum specific growth rate are fixed, and N uptake or excretion is determined by C and N mass balances. Although these Monod-type models have been quite useful for improving our understanding of microbial food webs, they prove difficult to use for detailed studies of bacterial DOM processing because they do not account for the variable energy content and oxidation state of DOM. Here we present a new, bioenergetically based model for describing bacterial utilization of DOM based on growth rate optimization subject to constraints on energy, redox reactions, substrate uptake kinetics, and the C:N ratio of bacteria.

It is well known that bacteria are primarily responsible for the processing of DOM in aquatic environments (Wright and Hobbie 1966; Azam and Hodson 1977) and that the efficiency with which bacteria utilize dissolved organic C (DOC) is an important factor governing the flow of C and energy through the microbial food web that leads to higher trophic levels (Azam et al. 1983; Ducklow et al. 1986; Sherr et al. 1987; Turner and Roff 1993). The extent to which dissolved organic N (DON) is reminer-

Acknowledgments

We are indebted to Ed Rastetter and Mat Williams for their comments during the preparation of this manuscript. We also appreciate the constructive criticism of David Kirchman and two anonymous reviewers.

This manuscript was supported by grants from the Lakian Foundation, the National Science Foundation Land Margin Ecosystems Research program (OCE 92-14461), and the DOE Ocean Margins Program (92-R6 1438).

alized or dissolved inorganic N (DIN) is immobilized by bacteria is also tightly coupled to DOM processing (Carlsson and Graneli 1993). Because phytoplankton directly compete with bacteria for DIN (Bratbak and Thingstad 1985; Stone 1990; Caron et al. 1988), it seems probable that the quality and quantity of DOM directly affects the dynamics of the entire food web, especially in estuarine and coastal environments, where allochthonous inputs are high. In this study, DOM quality refers to characteristics such as the C : N ratio, energy content, oxidation state, and the fraction of DOM that is labile (i.e. available to bacteria).

To assess how DOM is processed by microbial food webs, we must know the fraction of DOM subject to bacterial degradation over a characteristic time of interest (e.g. the residence time of an estuary or continental shelf), the rate of DOM consumption, the efficiency of DOC incorporation into bacterial biomass (i.e. bacterial C yield), and the extent of DON remineralization or DIN immobilization associated with DOM utilization. To quantify each of these processes for a particular ecosystem, the DOM must be characterized, for which two main approaches exist: chemical analysis and bioassay. Although significant improvements have been made in characterizing DOM by chemical analysis (Benner et al. 1992; Perdue 1984; Malcolm 1990), such techniques are currently unable to distinguish labile from refractory DOM. Consequently, microbial ecologists use bioassay techniques (Kirchman et al. 1991; Amon and Benner 1994) as the preferred method to determine biological availability of DOM.

Identification of the constituents, sources, and sinks of labile DOM is an active area of research. Low-molecular-weight compounds, such as amino acids, sugars, and organic acids, are readily assimilated by bacteria, as are easily degraded polymers (Amon and Benner 1994). Utilization of these low-molecular-weight compounds is the focus of our model. Production of these compounds by processes such as enzyme hydrolysis (Smith et al. 1992), ultraviolet radiation (Mopper et al. 1991), direct excretion (Williams 1990; Wood and van Valen 1990), sloppy feeding (Taylor et al. 1985), and cell lysis from viral attack (Steward et al. 1992) will not be considered in this study, although it is clear such processes are important (Billen et al. 1990).

To quantify many of the bacterial processes involved in DOM utilization, bioassay studies have been conducted to examine bacterial C yield (Kroer 1993; Linley and Newell 1984; Bjørnsen 1986; Goldman et al. 1987), N utilization (Tupas and Koike 1991; Jørgensen et al. 1993; Kirchman et al. 1989; Wheeler and Kirchman 1986; Goldman and Dennett 1991), and lability of DOM (Amon and Benner 1994; Kirchman et al. 1991) under a variety of environmental conditions. These studies have shown that bacterial C yield can range from $<5\%$ to $>90\%$ and that there is also a wide range of N utilization from both net N immobilization to net remineralization. However, owing to the lack of DOM chemical characterization, the causes of such significant variations in bacterial growth kinetics and growth processes remain unclear.

Because of the broad range of results that have been observed and the chemical complexity of DOM, conceptual models that attempt to describe general bacterial growth kinetics have been slow to develop. Most models for bacterial N processing are based on mass balance constraints that require knowledge of bacterial C yield (Goldman et al. 1987; Linley and Newell 1984). No models exist to predict bacterial C yield in natural environments, although such models have been developed for bacterial axenic cultures growing on defined medium (Heijnen and van Dijken 1992). As a result, most microbial food web models define bacterial yield as a constant, and either do not incorporate C and N coupling (Pace et al. 1984; Moran et al. 1988) or base such coupling on elemental balances only (Fasham et al. 1990; Taylor and Joint 1990; Moloney and Field 1991). Whether such simplifications are good approximations to reality depends on the focus of the study, but it is clear from bioassay experiments that these model "constants" are quite variable in nature. Furthermore, if a model is intended to examine the effects of DOM quality on its processing, then simple Monod-like growth models are inadequate.

Here, we do not examine a complete food web model, but rather focus entirely on bacterial utilization of DOM and DIN. The Monod-type expressions typically used to describe bacterial growth and nutrient uptake are replaced by a simple set of metabolic pathways that represent the processing of DOM and DIN into bacterial biomass. Reaction rates for the pathways are obtained by solving an optimization problem in which bacterial growth rate is maximized subject to constraints on energy, electron transfers, substrate kinetics, and biomass composition. This approach is similar to that developed by Anderson (1992), except a more generalized metabolism is used, redox reactions are accounted for, and the optimization problem eliminates the need to include numerous explicit equations for substrate preferences. The optimization approach itself is a rigorous implementation of the principles developed by Bloom et al. (1985) to explain resource limitations in plants. Similarities to Lassiter's (1986) work on ecosystem metabolism are also evident.

The model permits predictions of bacterial C yield, growth rate, and N processing. The model also is somewhat of a bridge between chemical and biological characterization of DOM in that basic information on DOM chemical characteristics is used to predict how bacteria will process the material. Results from our simulations employing various substrates indicate that the oxidation state of the substrate largely governs its processing by bacteria. Furthermore, the model demonstrates that bacterial growth cannot always be explained by a single constraint (such as the C : N ratio of the substrate), since resources are allocated such that several (or all) constraints are often active concurrently.

Model development

The model presented here focuses on bacterial utilization of DOM, nitrate, and ammonium for growth. DOM

is represented by three compartments: dissolved labile C and N (DLCN)-containing material, dissolved labile carbon (DLC)-containing material, and dissolved refractory C and N (DRCN)-containing material. An underlying rationale used in the model development is that the labile pools are made up of small molecules (or macromolecules that are easily hydrolyzed) that form the building blocks for bacterial biosynthesis. For simplicity, POM is not currently included in the model, but could be similarly represented in three compartments. The six compartments and their interconnections are illustrated in Fig. 1. Pathways leading from DRCN into the labile pools (DLCN and DLC) and the bacterial mortality pathway are specified by simple first-order kinetics and are only included for closure and for later integration into more complete food web models.

Metabolic reactions—Bacterial utilization of organic and inorganic nutrients is governed by a condensed set of metabolic reactions (Table 1) in which the rates ($\mathbf{r}_B$) are the desired unknowns. Mass balances are constructed for C and N flows only; however, C, H, O, and N composition of DOM is required to determine energy released from oxidation of the substrates and for balancing redox reactions (discussed below). If we view bacterial metabolism as a "black box," the DLCN pool (i.e. nitrogenous DOM) can be processed in four distinct ways: complete incorporation of both C and N into biomass (r_{B1}); incorporation of C, but excretion of N as NH_4^+ (r_{B2}); incorporation of N, but oxidation of C to CO_2 (r_{B3}); and complete oxidation of the compound to CO_2 and NH_4^+ (r_{B4}). Two similar reactions (r_{B5}, r_{B6}) represent bacterial utilization of the carbohydrate-like pool (DLC). Ammonium can be either incorporated into biomass (r_{B7}) or oxidized to nitrate (r_{B8}), whereas only one reaction is included for nitrate—incorporation into bacteria (r_{B9}). A respiratory reaction is also included (r_{B10}), but discussion of electron balancing is deferred until later. A final reaction is included to represent oxidation of stored bacterial reserves at the expense of bacterial biomass (r_{B11}). Although bacterial excretion of low-molecular-weight metabolites is possible (Jørgensen et al. 1993), the significance of such excretion in aquatic environments is unknown and is not represented here. We also give in Table 1 the vectors $\mathbf{r}_C$ and $\mathbf{r}_N$, which specify the amounts of C and N leading to bacterial biosynthesis per mole of substrate consumed.

To balance the stoichiometric reactions in Table 1, the elemental composition and the average molecular weight of the constituents that comprise DOM must be specified. Because most living organisms consist primarily of proteins, carbohydrates, nucleic acids, and lipids (Morowitz 1968; Ingraham et al. 1983), we can assume that labile material will similarly consist of such components and that the monomers that comprise these polymers will be likely candidates for transport across bacterial membranes and biosynthesis. Consequently, the nitrogenous pool (DLCN) represents material with a composition similar to that of amino acids and nucleic acids, and the nonnitrogenous pool (DLC) represents material with a composition similar to that of carbohydrates and lipids. For

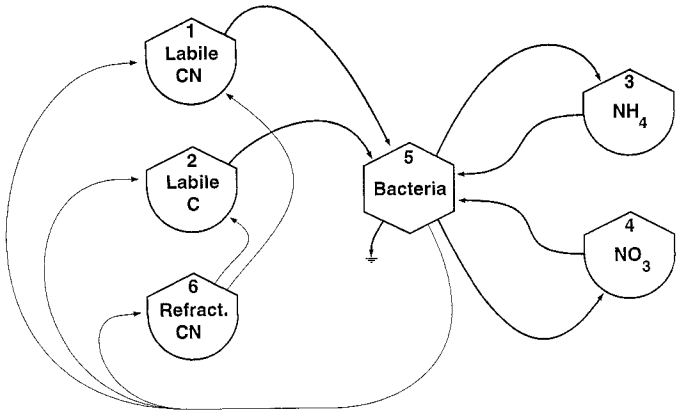

Fig. 1. Compartments and their interconnections associated with the bioenergetic model. The dissolved organic matter pools consist of (1) labile nitrogenous (DLCN), (2) labile carbohydrate (DLC), and (6) refractory nitrogenous (DRCN) materials. Pools 1–4 have fixed composition, whereas the composition of pools 5 (bacteria) and 6 are allowed to vary. Flows illustrated by heavy lines are determined by bioenergetics; other flows are given by first-order kinetics.

some simulations and as a point of reference, the composition of the DLCN pool and its free energy of formation ($\Delta G_f°$) (Table 2) are based on the average amino acid composition found in DOM (Zhang et al. 1992). Glucose is often used for the DLC pool; however, compositions of either pool can be manipulated to investigate growth on specific compounds or averaged mixtures, as will be demonstrated. The elemental composition of bacteria is similar among genera (Roels 1980); an average value is given in Table 2. The free energy of formation of a bacterial cell (Table 2) is from Morowitz (1968). The composition of DRCN (Table 2) is based on humic substances (Rashid 1985), but it does not play a significant role in the simulations presented here. To apply constraints to the reaction rates, we next determine both the change in free energy associated with each reaction and the requirements for electron acceptors or donors (i.e. redox balances).

Reaction redox and thermodynamics—The NAD^+/NADH half-reaction is used to balance all oxidation or reduction of substrates except for nitrification (r_{B8}), which is coupled directly to oxygen reduction. Oxygen is also used as the terminal electron acceptor in respiration (r_{B10}). Electron balancing is readily achieved when the reactants and products are well defined; however, a problem arises when dealing with poorly defined substrates, such as DOM and bacteria. To circumvent this problem, we compare the degree of reduction (ψ) of the substrates and products (in this case, bacteria) to determine the required number of electron transfers that must occur to balance the reaction. The degree of reduction of an organic compound is defined as the number of electrons transferred to oxygen when the substrate is oxidized to CO_2, H_2O, and NH_3 (Minkevich and Eroshin 1973). For a compound with elemental composition $C_\alpha H_\beta O_\gamma N_\delta$ and charge ξ, the degree of reduction is defined by

Table 1. Biochemical reactions for bacterial assimilation of organic and inorganic nutrients. Free energy of reaction (ΔG_r) and electron pair production (ΔE) are based on substrates given in Table 2 at 1 mM concentration and a thermodynamic efficiency, θ, of 20%. Also see Tables 3 and 5.

r_B	Description and stoichiometry*	r_C	r_N	ΔG_r (kJ mol^{-1})	ΔE (e^- pairs)
DLCN utilization					
r_{B1}	C and N incorporation				
	$C_{\alpha_1}H_{\beta_1}O_{\gamma_1}N_{\delta_1} + a\text{NAD}^+ \rightarrow \text{bacteria} + a\text{NADH} + a\text{H}^+$	α_1	δ_1	120	−0.26
r_{B2}	C incorporation, N excretion				
	$C_{\alpha_1}H_{\beta_1}O_{\gamma_1}N_{\delta_1} + a\text{NAD}^+ \rightarrow \text{bacteria} + \delta_1\text{NH}_4^+ + a\text{NADH} + (a - \delta_1)\text{H}^+$	α_1	0	288	−0.26
r_{B3}	C oxidation, N incorporation				
	$C_{\alpha_1}H_{\beta_1}O_{\gamma_1}N_{\delta_1} + a\text{NAD}^+ + b\text{H}_2\text{O} \rightarrow \text{bacteria} + \alpha_1\text{CO}_2 + a\text{NADH} + a\text{H}^+$	0	δ_1	−21.3	8.2
r_{B4}	C and N oxidation				
	$C_{\alpha_1}H_{\beta_1}O_{\gamma_1}N_{\delta_1} + a\text{NAD}^+ + b\text{H}_2\text{O} \rightarrow \alpha_1\text{CO}_2 + \delta_1\text{NH}_4^+ + a\text{NADH} + (a - \delta_1)\text{H}^+$	0	0	−5.74	9.4
DLC utilization					
r_{B5}	C incorporation				
	$C_{\alpha_2}H_{\beta_2}O_{\gamma_2} + a\text{NAD}^+ \rightarrow \text{bacteria} + a\text{NADH} + a\text{H}^+$	α_2	0	118	−0.60
r_{B6}	C oxidation				
	$C_{\alpha_2}H_{\beta_2}O_{\gamma_2} + a\text{NAD}^+ + b\text{H}_2\text{O} \rightarrow \alpha_2\text{CO}_2 + a\text{NADH} + a\text{H}^+$	0	0	−53.7	12.0
Ammonium utilization					
r_{B7}	Incorporation				
	$\text{NH}_4^+ + \text{NADH} + \text{H}^+ \rightarrow \text{bacteria} + \text{H}_2\text{O} + \text{NAD}^+$	0	1	−5.9	−1.0
r_{B8}	Oxidation (nitrification)				
	$\text{NH}_4^+ + 2\text{O}_2 \rightarrow \text{NO}_3^- + \text{H}_2\text{O} + 2\text{H}^+$	0	0	−69.6	0.0
Nitrate utilization					
r_{B9}	$\text{NO}_3^- + 5\text{NADH} + 6\text{H}^+ \rightarrow \text{bacteria} + 4\text{H}_2\text{O} + 5\text{NAD}^+$	0	1	−108	−5.0
Respiration					
r_{B10}	$\text{NADH} + \text{H}^+ + 1/2\text{O}_2 \rightarrow \text{NAD}^+ + \text{H}_2\text{O}$	0	0	−43.4	−1.0
Bacterial death (cellular oxidation)					
r_{B11}	$\text{Bacteria} + a\text{NAD}^+ + b\text{H}_2\text{O} \rightarrow \alpha_5\text{CO}_2 + \delta_5\text{NH}_4^+ + a\text{NADH} + (a - \delta_5)\text{H}^+$	$-\alpha_5$	$-\delta_5$	−19.4	10.5

* The stoichiometric coefficient a equals ΔE for the corresponding reaction.

$$\psi = 4\alpha + \beta - 2\gamma - 3\delta - \xi, \quad (1)$$

which reflects the valence states of the four elements. The degree of reduction has been used extensively in studies of bacterial stoichiometric growth (Roels 1983; Heijnen and van Dijken 1992) and represents the relative oxidation state of the compound. Often, the degree of reduction is reported on a per-C-mole basis, ψ_C, by dividing Eq. 1 by α, so that compounds of differing C content can be readily compared. For instance, the degree of reduction of methane is 8, whereas that of glucose is 4 per C mole. Additionally, it has been observed that ψ_C is similar for many different genera of bacteria and yeast, having a value of 4.2±0.13 per C mole (Minkevich and Eroshin 1973; Roels 1980). Furthermore, because ψ is based on a linear combination of elements and charge, it is a conserved quantity; that is, the degree of reduction summed over all substrates on the left-hand side of a reaction must equal that summed over the products on the right-hand side. Consequently, the number of electron pairs liberated (or required) by a reaction, defined here as ΔE, in which the substrate is completely converted to bacterial biomass is given by

$$\Delta E = \frac{1}{2}\left(\psi_i - \frac{\alpha_i}{\alpha_5}\psi_5\right). \quad (2)$$

The subscript 5 refers to bacteria, i to either DLCN or DLC, and α_i and ψ_i to the carbon content and degree of

Table 2. Chemical characteristics of compartments used as the standard reference case for the bioenergetic model (*see Fig. 1*).

Pool	Elemental composition	ΔG_r° (kJ mol^{-1})	ψ*
DLCN†	$C_{4.6}H_{9.2}O_{2.6}N_{1.2}$	−454	18.8
DLC (glucose)	$C_6H_{12}O_6$	−917	24
Ammonium	NH_4^+	−75.7	0
Nitrate	NO_3^-	−115	−8
Bacteria	$C_5H_9O_{2.5}N$	−345	21
DRCN	$C_{16.2}H_{24}O_8N$	−‡	−‡

* Degree of reduction (*see Eq. 1*).
† Average amino acid composition of protein.
‡ Not required for bioenergetics.

Table 3. Equations used to calculated electron transfer pairs, ΔE, for reactions given in Table 1. The quantities ΔE(I), ΔE(NR), and ΔE_C, represent electron transfers associated with N immobilization, nitrate reduction, and substrate oxidation, respectively.

$$\Delta E(r_{B1}) = \frac{1}{2}\left(\psi_1 - \frac{\alpha_1}{\alpha_5}\psi_5\right)$$

$$\Delta E(r_{B2}) = -\delta_1 \Delta E(I) + \frac{1}{2}\left(\psi_1 - 2\delta_1 - \frac{\alpha_1}{\alpha_5}\psi_5\right)^*$$

$$\Delta E(r_{B3}) = \Delta E_C(C_{\alpha_1}H_{\beta_1 - 3\delta_1}O_{\gamma_1+\delta_1}^{\zeta_1+})\dagger$$

$$\Delta E(r_{B4}) = \Delta E_C(C_{\alpha_1}H_{\beta_1}O_{\gamma_1}N_{\delta_1}^{\zeta_1+})$$

$$\Delta E(r_{B5}) = \frac{1}{2}\left(\psi_2 - \frac{\alpha_2}{\alpha_5}\psi_5\right)$$

$$\Delta E(r_{B6}) = \Delta E_C(C_{\alpha_2}H_{\beta_2}O_{\gamma_2}^{\zeta_2+})$$

$$\Delta E(r_{B7}) = \Delta E(I) = -1$$

$$\Delta E(r_{B8}) = 0$$

$$\Delta E(r_{B9}) = \Delta E(NR) + \Delta E(I) = (-4) + (-1) = -5\ddagger$$

$$\Delta E(r_{B10}) = -1$$

$$\Delta E(r_{B11}) = \Delta E_C(C_{\alpha_5}H_{\beta_5}O_{\gamma_5}N_{\delta_5}^{\zeta_5+})$$

$$\Delta E_C(C_{\alpha_i}H_{\beta_i}O_{\gamma_i}N_{\delta_i}^{\zeta_i+}) = (\beta_i + 4\alpha_i - 2\gamma_i - 3\delta_i - \xi_i)/2 = \psi_i/2$$

* Organic N remineralization is the opposite of NH_3 immobilization (r_{B7}); incorporated carbohydrate material has a degree of reduction of $\psi_1 - 2\delta_1$.

† Assumes N is removed by transamination, in which H-C-NH_2 is reversibly replaced by C=O, before compound is oxidized.

‡ NO_3 is first reduced to ammonium before immobilization.

reduction of the respective compounds. In effect, Eq. 2 represents the amount of NADH produced (or consumed for $\Delta E < 0$) to bring the substrate to the same degree of reduction as biomass per C mole. Equations for calculating ΔE for each reaction are given in Table 3.

The standard Gibbs free energy of reaction ($\Delta G_r°$, defined at pH 7.0 and 25°C for biochemical reactions) specifies the amount of energy (kJ mol^{-1}) that either can be harnessed for useful work ($\Delta G_r° < 0$, exergonic) or is required to drive a reaction forward ($\Delta G_r° > 0$, endergonic) when all the products and reactants are held constant at 1 M (except H^+ and H_2O). The standard free energy of reaction can be readily calculated from standard free energies of formation ($\Delta G_f°$) of the products (P_i) and reactants (R_j), as given by

$$\Delta G_r° = \sum_i \Delta G_f°(P_i) - \sum_j \Delta G_f°(R_j). \quad (3)$$

For reactions in which the products and reactants are not at 1 M, the standard free energy of reaction is augmented as

Table 4. Free energies of reaction associated with monomer polymerization for the macromolecular constituents of biomass calculated from group contribution methods (Mavrovouniotis 1991).

Macromolecule	Monomer	$\Delta G_r°$ (kJ mol^{-1})	TE* (%)	Cellular fraction
Protein	Amino acids	20	16	0.55 (f_P)
Lipid†	Fatty acid and glycerol	21	—	0.23 (f_F)
Carbohydrate	Glucose	24	31	0.10 (f_C)
Nucleic acid	Nucleotides	34	21	0.12 (f_N)

* Thermodynamic efficiency.

† Synthesis of fatty acids from acetate generates energy ($\Delta G_r° = -13.$ kJ mol^{-1}) but requires an electron pair. The energy released is not thought to be harnessed (so it is not included), and electron pair requirements are accounted for by Eq. 2.

$$\Delta G_r = \Delta G_r° + RT \ln \frac{\prod_i [P_i]}{\prod_j [R_j]}, \quad (4)$$

where $[P_i]$ and $[R_j]$ are product and reactant concentrations, R is the gas constant, and T is absolute temperature. The logarithmic term (Eq. 4) also accounts for energy expended in transporting substrates from the environment and into the cell (discussed below).

Examination of the reactions that lead to biomass synthesis reveals what seems to be a discrepancy between the left- and right-hand sides of these reactions (Table 1). Clearly, a mole of NH_4^+ alone cannot lead to a mole of bacteria (r_{B7}). This equation and the others involving biomass synthesis are intended to portray the incorporation of all or part of the substrate into "biomass." Consequently, the standard approach to obtain $\Delta G_r°$ (i.e. Eq. 3) cannot be applied. Instead, to calculate $\Delta G_r°$ for many of the reactions listed in Table 1, we used a group contribution method (Mavrovouniotis 1991) combined with knowledge of the biochemical reactions involved in substrate incorporation and the bulk composition of biomass. This approach is similar to that used by Morowitz (1968).

The energy associated with biomass synthesis is largely determined by the energy required for the transport of monomers across the cell membrane and their polymerization into the four macromolecular constituents of biomass (proteins, lipids, carbohydrates, and nucleic acids), since oxidation or reduction of monomers has already been accounted for (Table 3). Standard free energies of reaction associated with the polymerization of the four macromolecules, calculated by the group contribution method, are listed in Table 4 along with the fraction of bacterial biomass that they represent (Ingraham et al. 1983). The $\Delta G_r°$s for the biosynthetic reactions involving DLC and DLCN (r_{B1}, r_{B2}, and r_{B5}) are then determined by weighting the $\Delta G_r°$ for the polymerization reactions by the cellular fraction of each macromolecule (Table 4). The $\Delta G_r°$s for the oxidation reactions (r_{B3}, r_{B4}, r_{B6}, and r_{B11}) are calculated via Eq. 3, with NAD^+ as the electron

Table 5. Equations used to calculate free energies of reaction for reactions given in Table 1. The thermodynamic efficiency operator, Θ, is given by Eq. 6 and ΔG_T by Eq. 5.

$$\Delta G_r(r_{B1}) = \Theta\left[\Delta G_T(\mathrm{DLCN}) + \frac{f_P}{f_P + f_N}\Delta G_r^\circ(\mathrm{P}) + \frac{f_N}{f_P + f_N}\Delta G_r^\circ(\mathrm{N})\right]$$

$$\Delta G_r(r_{B2}) = \Theta\left[\Delta G_T(\mathrm{DLCN}) - \Delta G_r^\circ(\mathrm{I}) + \frac{f_C}{f_C + f_F}\Delta G_r^\circ(\mathrm{C}) + \frac{f_F}{f_C + f_F}\Delta G_r^\circ(\mathrm{F})\right]$$

$$\Delta G_r(r_{B3}) = \Theta[\Delta G_T(\mathrm{DLCN}) + \Delta G_C^\circ(\mathrm{C}_{\alpha_1}\mathrm{H}_{\beta_1 - 3\delta_1}\mathrm{O}_{\gamma_1+\delta_1}^{\zeta_1+})]^*$$

$$\Delta G_r(r_{B4}) = \Theta[\Delta G_T(\mathrm{DLCN}) + \Delta G_C^\circ(\mathrm{C}_{\alpha_1}\mathrm{H}_{\beta_1}\mathrm{O}_{\gamma_1}\mathrm{N}_{\delta_1}^{\zeta_1+})]$$

$$\Delta G_r(r_{B5}) = \Theta[\Delta G_T(\mathrm{DLC}) + f_P\Delta G_r^\circ(\mathrm{P}) + f_N\Delta G_r^\circ(\mathrm{N}) + f_C\Delta G_r^\circ(\mathrm{C}) + f_F\Delta G_r^\circ(\mathrm{F})]$$

$$\Delta G_r(r_{B6}) = \Theta[\Delta G_T(\mathrm{DLC}) + \Delta G_C^\circ(\mathrm{C}_{\alpha_2}\mathrm{H}_{\beta_2}\mathrm{O}_{\gamma_2}^{\zeta_2+})]$$

$$\Delta G_r(r_{B7}) = \Theta[\Delta G_T(\mathrm{NH_4}) + \Delta G_r^\circ(\mathrm{I})]$$

$$\Delta G_r(r_{B8}) = \Theta[\Delta G_T(\mathrm{NH_4}) + \Delta G_r^\circ(\mathrm{AO})]$$

$$\Delta G_r(r_{B9}) = \Theta[\Delta G_T(\mathrm{NO_3}) + \Delta G_r^\circ(\mathrm{NR}) + \Delta G_r^\circ(\mathrm{I})]$$

$$\Delta G_r(r_{B10}) = \Theta[\Delta G_r^\circ(\mathrm{R})]$$

$$\Delta G_r(r_{B11}) = \Theta[\Delta G_C^\circ(\mathrm{C}_{\alpha_5}\mathrm{H}_{\beta_5}\mathrm{O}_{\gamma_5}\mathrm{N}_{\delta_5}^{\zeta_5+})]$$

$$\Delta G_C^\circ(\mathrm{C}_{\alpha_i}\mathrm{H}_{\beta_i}\mathrm{O}_{\gamma_i}\mathrm{N}_{\delta_i}^{\zeta_i+}) = \alpha_i\Delta G_f^\circ(\mathrm{CO_2}) + \delta_i\Delta G_f^\circ(\mathrm{NH_4^+}) + \frac{\psi_i}{2}\Delta G_r^\circ(\mathrm{NAD^+} \rightarrow \mathrm{NADH}) + \left(\frac{\psi_i}{2} - \delta_i + \xi_i\right)\Delta G_f^\circ(\mathrm{H^+}) - [\Delta G_f^\circ(\mathrm{C}_{\alpha_i}\mathrm{H}_{\beta_i}\mathrm{O}_{\gamma_i}\mathrm{N}_{\delta_i}^{\zeta_i+}) + (2\alpha_i - \gamma_i)\Delta G_f^\circ(\mathrm{H_2O})]$$

$\Delta G_r^\circ(\mathrm{NAD^+} \rightarrow \mathrm{NADH})$: NAD^+ conversion to NADH (19.8 kJ mol^{-1})†

$\Delta G_r^\circ(\mathrm{I})$: Ammonium immobilization (−29.5 kJ mol^{-1})†

$\Delta G_r^\circ(\mathrm{NR})$: Nitrate reduction to ammonium by NADH (−512 kJ mol^{-1})†

$\Delta G_r^\circ(\mathrm{AO})$: Ammonium oxidation to nitrate by O_2 (−348 kJ mol^{-1})

$\Delta G_r^\circ(\mathrm{R})$: Oxidation of NADH to NAD^+ by O_2 (−271 kJ mol^{-1})†

$\Delta G_f^\circ(\mathrm{CO_2})$: Formation energy of CO_2 (−394.6 kJ mol^{-1})

$\Delta G_f^\circ(\mathrm{HN_4^+})$: Formation energy of NH_4^+ (−75.73 kJ mol^{-1})

$\Delta G_f^\circ(\mathrm{H_2O})$: Formation energy of H_2O (−236.8 kJ mol^{-1})

$\Delta G_f^\circ(\mathrm{H^+})$: Formation energy of H^+ (−39.75 kJ mol^{-1})

* $\Delta G_f^\circ(\mathrm{C}_{\alpha_1}\mathrm{H}_{\beta_1-3\delta_1}\mathrm{O}_{\gamma_1+\delta_1}^{\zeta_1+} = \Delta G_f^\circ(\mathrm{DLCN}) - 115.9\delta_1$.

† Obtained by group contribution method.

acceptor (not O_2). Ammonium immobilization (r_{B7}) proceeds by reductive amination of α-oxoglutarate, where the ΔG_r° is obtained via the group contribution method. The ΔG_r° for nitrification (r_{B8}) is calculated directly via Eq. 3. Nitrate assimilation (r_{B9}) proceeds first by reduction to NH_4^+, where the ΔG_r° is obtained by the group contribution method, and then by immobilization (as for r_{B7}). The equations for calculating ΔG_r for the 11 metabolic reactions for a given substrate C, H, O, and N composition and charge are summarized in Table 5; however, these equations have been modified to account for transport and thermodynamic efficiency.

Free energy change associated with metabolite transport across the cell membrane (ΔG_T) is given by Eq. 4, with ΔG_r° set to zero and $[P_i]$ and $[R_j]$ replaced by the intracellular and extracellular substrate concentrations, respectively. Because the concentration of many intracellular metabolites is in the millimolar range (Simon and Azam 1989) and the concentration of extracellular substrates is in the nanomolar range (Billen et al. 1980), metabolites are typically concentrated by a factor of $\sim 10^6$, resulting in a free energy change of 34 kJ mol^{-1} at 20°C (for comparison, hydrolysis of 1 mol ATP releases 30.5 kJ). In the model, intracellular concentrations of all substrates are held at 1 mM, while extracellular concentrations are free to vary. We therefore assume

$$\Delta G_T(E_j) = RT \ln\left(\frac{1{,}000}{[E_j]}\right), \tag{5}$$

where $[E_j]$ is the extracellular concentration of metabolite E_j in μM.

The free energy of reaction specifies the amount of energy that *can* be harnessed for useful work if the process (i.e. reaction) is run reversibly. However, ΔG_r does not specify the *actual* energy the cell recovers from exergonic reactions or the energy expended to drive endergonic reactions. Comparison between the calculated $\Delta G_r°$ for the polymerization reactions and the actual energy expended by the cell, obtained from actual ATP requirements (Stouthamer 1973), reveals thermodynamic efficiencies of 15–30% (Table 4). Consequently, the actual energy required or recovered from a biochemical reaction is given by the following thermodynamic efficiency operator:

$$\Theta(\Delta G_r) = \begin{cases} \Delta G_r \theta & \text{for} \quad \Delta G_r \leq 0 \\ \dfrac{\Delta G_r}{\theta} & \text{for} \quad \Delta G_r > 0 \end{cases}. \tag{6}$$

θ is the thermodynamic efficiency, which is held constant in the model at 0.2 for all reactions. Because the Θ operator is not distributive [i.e. $\Theta(a + b) \neq \Theta(a) + \Theta(b)$], it is always applied to each step in a series of reactions before addition, so that $\Theta(\Delta G_{r1} \pm \Delta G_{r2})$ is converted to $\Theta(\Delta G_{r1}) \pm \Theta(\Delta G_{r2})$.

Reaction constraints and optimization—The basis of the bioenergetic model is maximization of bacterial growth rate, which is governed by the metabolic reaction rates (Table 1). However, the selection of the reaction rates must comply with physics and our understanding of bacterial growth. In this section, reaction constraints dictated by substrate kinetics, energy balance, electron conservation, and the bacterial C : N ratio are developed, and the optimization function for bacterial growth rate is defined.

Total uptake rates of substrates from the environment are limited by enzyme kinetics and the concentrations of bacteria and substrates. Monod-type growth kinetics are typically used to specify the biomass specific uptake rate of a limiting substrate (Taylor and Joint 1990; Fasham et al. 1990). A similar approach is taken here, except that the kinetic expressions do not limit growth directly, but instead limit the biochemical reaction rates associated with the particular substrate. These kinetic constraints on the reaction rates are given as

$$r_{B1} + r_{B2} + r_{B3} + r_{B4} \leq \frac{a_1(t)[\text{DLCN}]}{k_{1,5} + [\text{DLCN}]}[\text{bacteria}] \tag{7}$$

$$r_{B5} + r_{B6} \leq \frac{a_2(t)[\text{DLC}]}{k_{2,5} + [\text{DLC}]}[\text{bacteria}] \tag{8}$$

$$r_{B7} + r_{B8} \leq \frac{a_3(t)[\text{NH}_4^+]}{k_{3,5} + [\text{NH}_4^+]}[\text{bacteria}] \tag{9}$$

$$r_{B9} \leq \frac{a_4(t)[\text{NO}_3^-]}{k_{4,5} + [\text{NO}_3^-]}[\text{bacteria}], \tag{10}$$

where $k_{i,5}$ is the half-saturation constant for the corresponding substrate, $a_i(t)$ is the allocated maximum uptake rate per unit of bacterial biomass at time t associated with each substrate, and [bacteria] is the concentration of bacteria. Fixed maximum uptake rates in the kinetic constraints are not used because organisms are able to allocate resources (i.e. uptake and processing pathways) to substrates that enhance growth rate (Rastetter and Shaver 1992; Bloom et al. 1985). Diauxic—or biphasic—growth observed in bacteria is a result of such reallocation of enzymatic systems (Gottschalk 1986). These four allocation variables $[a_1(t), \ldots a_4(t)]$ are not specified by the user or environment, but rather become auxiliary variables that are adjusted to maximize growth rate in the optimization problem. However, the total resources available to bacteria are not unlimited, so the a_i for the four bacterial substrates are constrained by

$$\sum_{i=1}^{4} a_i(t) \leq a_{\max}, \tag{11}$$

where $a_{\max}$ specifies the maximum resources per bacterial biomass that can be allocated and is set so that the resulting bacterial growth rate is consistent with observations.

The reallocation of resources cannot occur instantaneously (time is required for DNA transcription, protein synthesis, etc.), so upper and lower bounds on the *rate* at which resources can be reallocated (i.e. da_i/dt) are placed on each allocation variable as

$$a_i(t - \tau) - \left|\tau \frac{a_{\max}}{\omega}\right| \leq a_i(t) \leq a_i(t - \tau) + \left|\tau \frac{a_{\max}}{\omega}\right|, \quad i = 1, 2, 3, 4. \tag{12}$$

ω is the time required to reallocate all resources, and τ specifies the increment between iterations. Presently, the respiration reaction r_{B10} is not constrained by kinetics in the standard model, but this can easily be modified if oxygen limitations are imposed.

Reaction rates are constrained such that energy liberated from the exergonic reactions must be greater than or equal to the energy consumed by the endergonic (i.e. biosynthetic) reactions and maintenance, as given by

$$\sum_{i=1}^{11} r_{Bi}\Theta(\Delta G_{ri}) \leq m_e[\text{bacteria}], \tag{13}$$

where m_e is the maintenance coefficient for bacteria, and Θ is the thermodynamic efficiency operator given by Eq. 6. Similarly, electron acceptors and donors summed over all reactions must balance exactly, so that

$$\sum_{i=1}^{11} r_{Bi}\Delta E_{ri} = 0. \tag{14}$$

Although the C : N ratio for bacteria is not constant, it does not vary beyond observed limits for viable cells. Consequently, the relative C and N rates of biosynthesis must be constrained between lower and upper bounds. The rate of bacterial C synthesis is given by $\mathbf{r}_C^T\mathbf{r}_B$, while

Table 6. State equations for bioenergetic model.

$$\dot{C}_1(t) = \frac{\alpha_1}{\delta_1} f^{N}_{5,1} m_b N_5(t) + \frac{\alpha_1}{\delta_1} d^{N}_{6,1} N_6(t) - \alpha_1[r_{B1}(t) + r_{B2}(t) + r_{B3}(t) + r_{B4}(t)]^*$$

$$\dot{N}_1(t) = f^{N}_{5,1} m_b N_5(t) + d^{N}_{6,1} N_6(t) - \delta_1[r_{B1}(t) + r_{B2}(t) + r_{B3}(t) + r_{B4}(t)]$$

$$\dot{C}_2(t) = \left(1 - \frac{\alpha_1 N_5(t)}{\delta_1 C_5(t)} f^{N}_{5,1} - f^{C}_{5,6}\right) m_b C_5(t) + d^{C}_{6,2} C_6(t) - \alpha_2[r_{B5}(t) + r_{B6}(t)]^\dagger$$

$$\dot{N}_3(t) = \delta_1[r_{B2}(t) + r_{B4}(t)] + \delta_5 r_{B11}(t) - [r_{B7}(t) + r_{B8}(t)]$$

$$\dot{N}_4(t) = r_{B8}(t) - r_{B9}(t)$$

$$\dot{C}_5(t) = \alpha_1[r_{B1}(t) + r_{B2}(t)] + \alpha_2 r_{B5}(t) - \alpha_5 r_{B11}(t) - m_b C_5(t)$$

$$\dot{N}_5(t) = \delta_1[r_{B1}(t) + r_{B3}(t)] - \delta_5 r_{B11}(t) - m_b N_5(t)$$

$$\dot{C}_6(t) = f^{C}_{5,6} m_b C_5(t) - \frac{\alpha_1}{\delta_1} d^{N}_{6,1} N_6(t) - d^{C}_{6,2} C_6(t)$$

$$\dot{N}_6(t) = (1 - f^{N}_{5,1}) m_b N_5(t) - d^{N}_{6,1} N_6(t)$$

* Enough C accompanies N from bacterial and DRCN decomposition to preserve C : N stoichiometry of the DLCN pool (first two terms of eq.).

† Excess C associated with bacterial decomposition is partitioned into the DLC pool (first term in eq.).

that for N biosynthesis is $\mathbf{r}_N^T \mathbf{r}_B$ (the vectors $\mathbf{r}_C$ and $\mathbf{r}_N$ are listed in Table 1). The composition constraints are given by

$$\rho_L \le \frac{\mathbf{r}_C^T \mathbf{r}_B}{\mathbf{r}_N^T \mathbf{r}_B} \le \rho_U \quad \text{or} \quad \begin{cases} (\mathbf{r}_C^T - \rho_U \mathbf{r}_N^T)\mathbf{r}_B \le 0 \\ (\mathbf{r}_C^T - \rho_L \mathbf{r}_N^T)\mathbf{r}_B \ge 0 \end{cases}, \tag{15}$$

where ρ_U and ρ_L are the upper and lower bounds on the bacterial C : N ratio.

For a given set of substrate and bacterial concentrations, solutions for the reaction rates ($\mathbf{r}_B(t)$; Table 1) and allocation variables ($\mathbf{a}(t)$, Eq. 7–10) can be obtained by maximizing bacterial C and N biosynthesis rates subject to the constraints outlined by Eq. 7–15. Because all functions are linear, the optimization is implemented by setting up the following linear programming (LP) problem:

$$\underset{\mathbf{r}_B, \mathbf{a}}{\text{Maximize:}} \ (\mathbf{r}_C^T + \rho_B \mathbf{r}_N^T)\mathbf{r}_B$$

$$\text{Subject to: } \mathbf{A}\begin{bmatrix} \mathbf{r}_B \\ \mathbf{a} \end{bmatrix} \le \mathbf{c} \quad \text{and} \quad \begin{bmatrix} \mathbf{r}_B \\ \mathbf{a} \end{bmatrix} \ge 0. \tag{16}$$

The matrix $\mathbf{A}$ and vector $\mathbf{c}$ represent the constraints embodied in Eq. 7–15, and ρ_B is the average C : N ratio for bacteria. The solution to the LP problem (Press et al. 1986) provides the 11 reaction rates (Table 1) that replace the simple Monod-like growth equations, as well as similar substrate consumption approximations, used in most bacterial growth models.

State equations—To complete the bacterial growth model, a standard state model is constructed from C and N balances around each of the six compartments following the connections illustrated in Fig. 1. The C, H, O, and N compositions of the DLCN, DLC, NH_4^+, and NO_3^- pools are maintained at their initial values (Table 2), whereas the compositions of the DRCN and bacterial compartments are allowed to vary. Two flows that are not obtained from solution of the LP problem are the mortality of bacteria and the decomposition of DRCN into the DLCN and DLC pools. When C_i and N_i represent the C and N concentrations (μM) in compartment i of Fig. 1, the state model is given by the set of differential equations listed in Table 6. In these equations, bacterial mortality occurs via first-order kinetics, governed by the rate constant m_b, and is partitioned into the three organic matter compartments. Similarly, the decomposition of the DRCN pool into the DLCN and DLC pools is also governed by first-order kinetics as specified by $d^{N}_{6,1}$ and $d^{C}_{6,2}$. All other flows are governed by the solution to the linear programming problem (Eq. 16).

The algorithm implemented to obtain a solution of the state variables at various increments is as follows. At time t, the linear programming problem (Eq. 16) is solved based on the current concentrations of the state variables, $\mathbf{C}(t)$ and $\mathbf{N}(t)$. The reaction rates obtained from the optimization, $\mathbf{r}_B(t)$, are used to set most of the flows in the state model (Table 6), which is integrated forward in time to obtain the concentration of the state variables at $t + \Delta t$, thereby completing one iteration. Fortran routines from the SLATEC library (National Energy Software Center, Argonne, Illinois) were used to integrate the state space model and solve the linear programming problem. These routines were obtained from Netlib (Dongarra and Grosse 1987).

Parameter values—Parameter values used for all simulations (Table 7) were chosen to be close to values typically observed for bacterial populations found in natural environments. The maximum resource allocation value, a_{max}, of 6.0 d^{-1} was chosen to be intermediate between maximum growth rates observed for natural populations (typically 0.7 d^{-1}) and those observed for laboratory cultures (often >16 d^{-1}). The bacterial maintenance coef-

ficient, m_e, is based on the lower range of values found for bacteria and yeast (Stouthamer 1978).

Each of the simulations presented below is run in a batch mode (i.e. no advection or diffusion), so that substrates soon become exhausted. Conducting simulations in batch mode forces the model to adjust to continuously changing environments in one run. In order for results from the growth model to be easily analyzed, bacterial mortality, m_B, has been set to zero and the concentration of the refractory DOM (i.e. DRCN) has also been initialized to zero in all runs.

Results

In this section we present results from a variety of simulations in which environmental conditions (i.e. compartment concentrations and compositions) have been varied or model parameters have been modified. Some of these simulations were conducted to examine how the model responds to a particular set of conditions, such as DON limitation, while other simulations represent interesting results observed during the course of model development. The first two simulations investigate the effects of changing the relative concentrations of the DLCN and DLC pools. Simulations 3 and 4 illustrate an interesting result in which the model switches from a high substrate uptake, low-yield mode to a low substrate uptake, high-yield mode when the half-saturation constant for DLCN uptake is increased. The last set of simulations examines the effects of changing the degree of reduction of the substrate.

Manipulations of the labile DOM C : N ratio—The first two simulations examine the general response of the model to different concentrations of the DLC and DLCN pools, which affects the C : N ratio of the bulk labile pool and, hence, N cycling. In both cases, glucose is used as the representative compound for the labile carbohydrate pool (DLC), while the bulk composition of an aggregated pool of amino acids is used to represent the DLCN pool, as given in Table 2. The first simulation (Fig. 2) shows the response of the model when the initial concentration of DLCN is greater than DLC, so that the total labile pool C : N ratio is 4.8. During the first part of the simulation, both DOM substrates are consumed concurrently (Fig. 2A, 0–0.25 d), but are processed differently. During this period, all DLCN consumed is incorporated into biomass (r_{B1}), while DLC is mostly used for energy production (r_{B6}), although just enough C is incorporated into biomass to satisfy bacterial C : N constraints (Fig. 2C). The ratio of C to N incorporation throughout the simulation is maintained at the lower bound, ρ_L, so that the average bacterial C : N ratio decreases continuously (Fig. 2B).

Near the point of DLC exhaustion (~0.25 d), resource allocations shift to the uptake of DLCN only. This switching is accompanied by decreases in specific growth rate and yield (Fig. 2B) and is reminiscent of diauxic growth behavior (Gottschalk 1986). During the transition, the oxidation of DLC is replaced by complete oxidation and N remineralization of DLCN (r_{B4} and r_{B2}; Fig. 2C), which results in the accumulation of NH_4^+ (Fig. 2A). This mode of operation continues until the exhaustion of DLCN. Near the end of the simulation, nitrification (r_{B8}) commences, which results in the accumulation of NO_3^- at the expense of NH_4^+ (Fig. 2A, D). Nitrification does not occur before this time because of its poor energy yield; resources allocated to this process would not give the greatest possible return. This is not to imply that heterotrophic nitrifiers exist. The nitrification reaction was added to examine the conditions under which nitrification might occur.

In the next simulation, the relative concentrations of DLCN and DLC are reversed, so that the labile pool C : N ratio is 29 (Fig. 3). As before, when both substrates are present, both DLC and DLCN are taken up concurrently with identical processing, growth rate, and yield. However, the transition that accompanies DLCN exhaustion (Fig. 3A at ~0.2 d) differs significantly from the previous simulation. At the transition, DLCN incorporation is replaced by DLC incorporation and oxidation (r_{B5} and r_{B6}) coupled with NH_4^+ immobilization (r_{B7}, Fig. 3C, D). This mode proceeds until near NH_4^+ exhaustion (~0.63 d), at which time NO_3^- uptake commences (r_{B9}). During this transition, there is a brief period when assimilation of both NO_3^- and NH_4^+ occurs (Fig. 3D). The two reallocation periods are also reflected in changes in growth rate and yield, as well as a change in the trend of the bacterial C : N ratio following exhaustion of DLCN (Fig. 3B). Such trends in the bacterial C : N ratio are consistent with observations on bacterial growth during periods of C limitation, N limitation, or co-limitations (Egli 1991; Goldman and Dennett 1991). Near the end of the simulation, following DLC exhaustion, oxidation of bacterial biomass is observed (r_{B11}; Fig. 3D).

Table 7. Parameter values used in simulations unless otherwise noted in text.

Parameter	Value	Description
θ	0.2	Thermodynamic efficiency (dimensionless)
m_e	50	Bacteria maintenance energy (kJ mol^{-1} d^{-1})
a_{max}	6.0	Maximum resource allocation (d^{-1})
ω	1	Total reallocation time (d)
$k_{1,5}$	0.1	Half-saturation constant for DLCN uptake (μM)
$k_{2,5}$	0.1	Half-saturation constant for DLC uptake (μM)
$k_{3,5}$	0.1	Half-saturation constant for NH_4^+ uptake (μM)
$k_{4,5}$	0.1	Half-saturation constant for NO_3^- uptake (μM)
ρ_B	5.0	Bacterial C : N ratio
ρ_U	5.2	Upper bound on bacterial C : N ratio
ρ_L	4.8	Lower bound on bacterial C : N ratio
m_B	0	Bacterial mortality rate (d^{-1})
$f^N_{5,1}$	0.8	Fraction of bacterial N to DLCN pool
$f^C_{5,6}$	0.1	Fraction of bacterial C to DRCN pool
$d^N_{6,1}$	0.001	Decomposition of DRCN into DLCN
$d^C_{6,2}$	0.001	Decomposition of DRCN into DLC

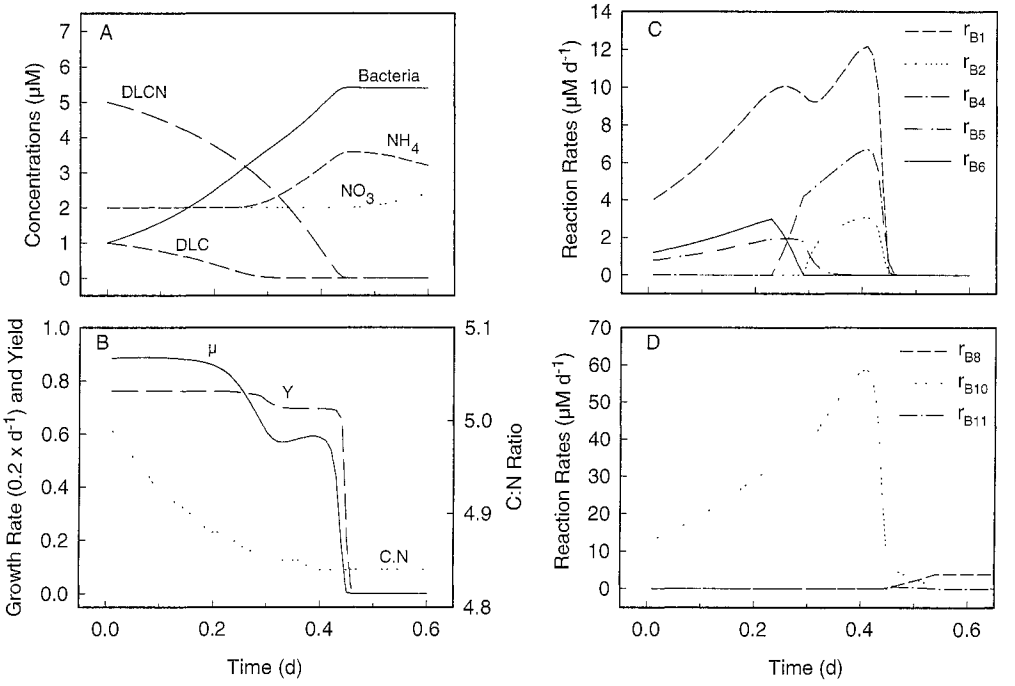

Fig. 2. Simulation 1 initialized with low concentration (1 μM) of glucose (DLC) and high concentration (5 μM) of an amino acid mixture (DLCN, Table 2). Unless otherwise noted, bacteria, ammonium (NH_4^+), and nitrate (NO_3^-) concentrations are initialized at 1, 2, and 2 μM, respectively. A. Concentrations of state variables whose compositions are given in Table 2. B. Specific, C-based growth rate (μ), bacterial carbon yield (Y, mol C bacteria/mol C consumed), and bacterial C : N ratio (atomic). C, D. Reaction rates (μmol liter^{-1} d^{-1}), based on stoichiometry given in Table 1, for reactions involved with DLCN (r_{B1}–r_{B4}) and DLC (r_{B5}, r_{B6}) uptake (C) and ammonium (r_{B7}, r_{B8}) and nitrate (r_{B9}) uptake, respiration (r_{B10}), and bacterial oxidation (r_{B11}) (D). Model parameters are given in Table 7.

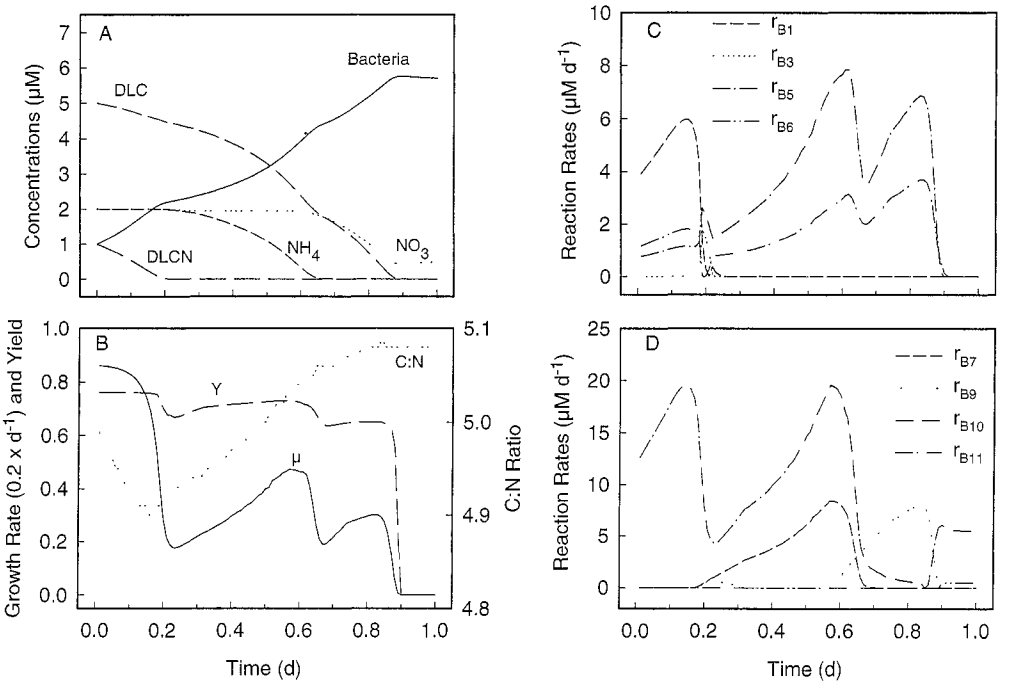

Fig. 3. Simulation 2 initialized with a high concentration (5 μM) of glucose (DLC) and a low concentration (1 μM) of amino acid mixture (DLCN). See caption of Fig. 2 for details.

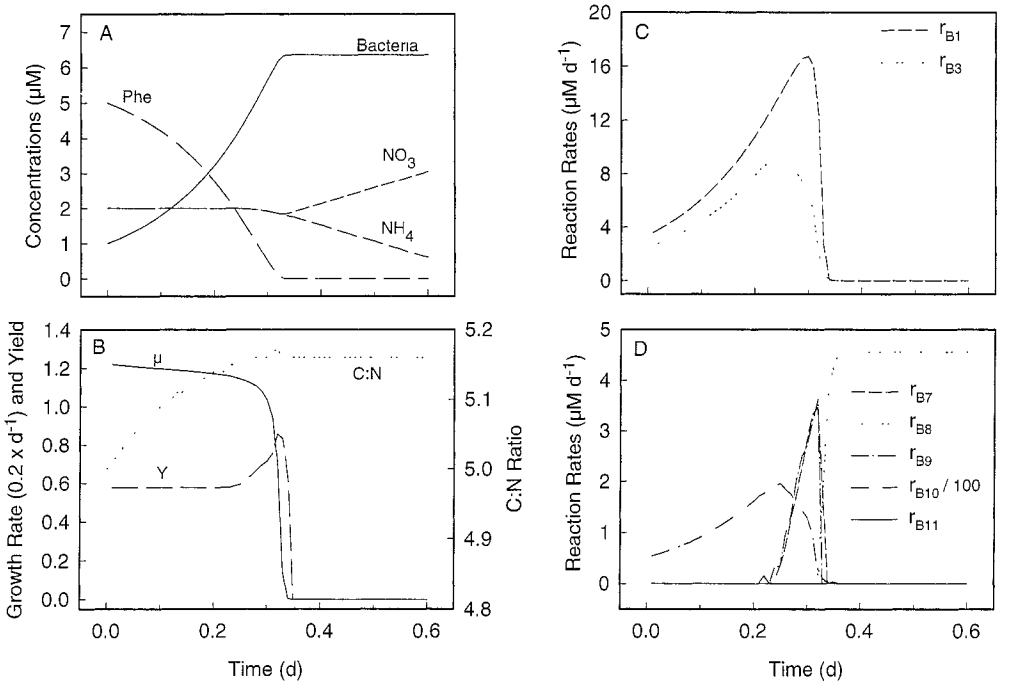

Fig. 4. Simulation 3 with phenylalanine (Phe) as the only C-containing substrate. Other conditions as given in the caption of Fig. 2.

During the initial phase of each simulation, while both substrates are present, N is neither immobilized nor remineralized, even though the bulk C : N ratio of the aggregated labile pools is 4.8 for the first simulation and 29 for the second simulation. Eventually, N is remineralized or immobilized, as is expected from simple mass balances (Goldman et al. 1987; Linley and Newell 1984) for batch processes. However, if the simulations were conducted for a chemostat under conditions where neither substrate is exhausted, N immobilization or remineralization would not occur. Such co-substrate processing, which seems to occur to some extent in nature (Kirchman et al. 1989; Goldman and Dennett 1991; Egli et al. 1993), can be important for N dynamics in environments subject to strong advection, such as rivers and estuaries. It is also clear from these two simulations that amino acids are the preferred N source. Experimental support for this observation is still unclear (Goldman and Dennett 1991; Kirchman et al. 1989; Kirchman 1990).

Optimality and yield—An interesting result observed in model simulations is the sensitivity of bacterial growth kinetics to slight changes in environmental conditions or growth parameters. To illustrate the phenomena, phenylalanine (Phe) is used as the DLCN source without any DLC substrate. In this simulation, with the standard set of model parameters (Table 7), Phe is initially solely consumed at a rapid rate, producing a higher growth rate than in previous runs, but at a reduced yield (Fig. 4). After exhaustion of Phe, nitrification explains the increase of NO_3^- at the expense of NH_4^+. An interesting phenomenon occurs near the point of Phe exhaustion at 0.3 d. As Phe becomes limiting, bacterial yield begins to increase significantly and both NO_3^- and NH_4^+ are consumed (Fig. 4). To examine this change in more detail, we ran another simulation in which the half-saturation constant for DLCN uptake ($k_{1,5}$) was increased to 1.0 μM, thereby increasing the resistance to (or constraint on) Phe uptake. With this relatively minor change, a significant alteration in metabolism occurs (Fig. 5). In contrast to the first run, Phe uptake rate is greatly reduced and is accompanied by DIN uptake. Furthermore, growth rate is slightly reduced from 6.1 to 5.4 d^{-1}, but there is a sizable increase in yield from 58 to 88% (Figs. 4B, 5B), which is evident in the greater final bacterial concentration.

This increase in yield can be explained by the high C : N ratio for Phe (C : N of 9, which is at the upper bound for the standard amino acids). Because this C : N ratio is significantly higher than that of bacteria (ρ_B = 5), one approach to optimality is to place all resources on Phe incorporation (r_{B1}) and C-only oxidation (r_{B3}), so that the C : N ratio of the resulting material conforms with the constraints on bacterial C : N ratio. This approach results in low bacterial yield, but so long as Phe can be consumed at a high rate, it is the optimal choice for maximizing growth rate when Phe uptake is saturated. The situation changes, however, when Phe becomes limiting, as in the second simulation. In this case, optimality involves allocation of some resources to DIN uptake to effectively reduce the C : N ratio of Phe. Phe uptake rate is lower owing to allocation of some resources to DIN uptake, but because of the secondary source of N, more Phe-C can be retained in biomass, thereby enhancing yield.

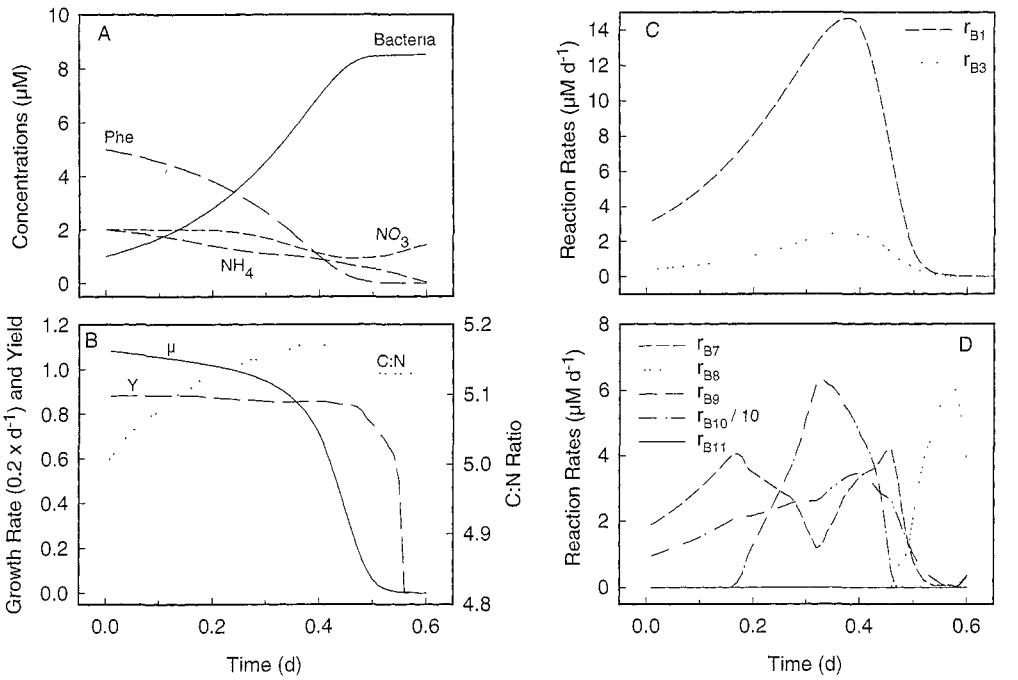

Fig. 5. Simulation 4: Same as simulation 3 of Fig. 4, except the half-saturation constant for Phe uptake, $k_{1,5}$, has been increased from the nominal value of 0.1 μM to 1.0 μM.

It is clear from these two simulations that resource allocation plays a crucial role in the model. The transition from low yield to high yield occurs when resources allocated to Phe uptake can be better utilized for DIN consumption. This transition also occurs in the dynamics of DIN uptake. In the second simulation (Fig. 5A, D), NH_4^+ uptake is partially replaced by NO_3^- consumption for a significant portion of the simulation. This change occurs because for a given DIN uptake rate fewer resources have to be allocated to NO_3^- uptake than to NH_4^+ uptake when the former is at a higher concentration and the half-saturation constants for both nutrients are the same. At a certain threshold, the reduction in resources for DIN uptake associated with NO_3^- more than offsets the greater energy cost in NO_3^- assimilation.

The switch in Phe uptake modes is a direct consequence of maximizing the rate of growth instead of energy efficiency. Although the two optimization strategies often overlap, maximizing growth rate can lead to preferential uptake of a less desirable substrate if the substrate can be consumed at a significantly higher rate than can an energy-rich substrate. The main point illustrated by these two simulations is that slight changes in uptake kinetics, which may result from changes in population structures or substrate concentrations, can significantly affect the processing of organic matter and DIN.

Degree of substrate reduction—Because organic compounds have different elemental compositions, we ran a set of simulations to examine the effect of substrate reduction (defined by Eq. 1) on bacterial growth kinetics. The first compound examined, glycollate ($C_2H_3O_3^-$; ψ_C = 2.0), is more oxidized than is glucose (ψ_C = 4.0) or bacteria (ψ_B = 4.2). Glycollate is ecologically important in that it is a typical, if not dominant, phytoplankton exudate (Marlowe et al. 1989; Fogg 1983). To complement glycollate, we used the average amino acid mixture (Table 2) at low concentration for the DLCN compartment; all other parameters were kept at their previous values (Table 7).

Results from the simulation (Fig. 6) show that processing of glycollate differs significantly from that of glucose (Fig. 3). Unlike glucose, glycollate is not utilized while DLCN is present, so that DLCN-N is remineralized at the start of the simulation (Fig. 6A,C). Following DLCN depletion, uptake switches to glycollate, but the resulting growth rate and yield are substantially reduced, and the bacterial C : N ratio continues toward its lower bound (Fig. 6B). These results indicate that the degree of reduction of a substrate may significantly affect bacterial growth. To examine this effect further, we ran another simulation involving urea.

In this simulation, urea was used as the DLCN substrate (CH_4ON_2; ψ_C = 0) and glucose as the DLC source at low concentration (Fig. 7). During the first part of the simulation when glucose is present, urea is consumed as the preferred N source, over NH_4^+, and growth rate and yield are high, as in previous simulations. Bacterial C in this period comes solely from glucose, since the urea-C is oxidized (Fig. 7C, r_{B3}). Following glucose depletion, growth rate and yield drop to zero because urea does not provide enough energy for growth; this is consistent with observations (Goldman et al. 1987). Examination of the metabolic reactions reveals that complete oxidation of

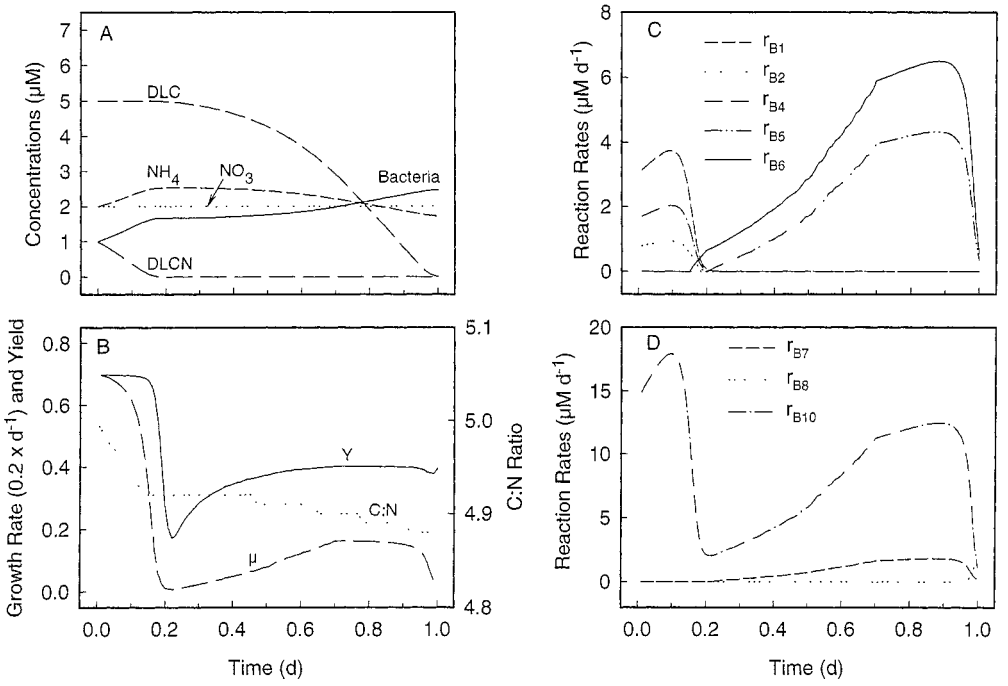

Fig. 6. Simulation 5, with glycollate as the DLC source and the amino acid mixture as the DLCN source (Table 2). Other conditions as given in the caption of Fig. 2.

urea (r_{B4}) is the dominant pathway immediately following glucose depletion, which explains the initial accumulation of NH_4^+. As the simulation proceeds, complete oxidation of urea is slowly replaced by N remineralization from urea (r_{B2}), slight urea incorporation into biomass (r_{B1}), and a high rate of nitrification (r_{B8}). From this combination of reactions, NH_4^+ is both consumed and produced at the same time (r_{B4} and r_{B8}).

To more thoroughly investigate the impact that substrate oxidation has on bacterial yield and growth rate, we conducted a series of simulations with individual substrates (Table 8). For each simulation, the initial substrate

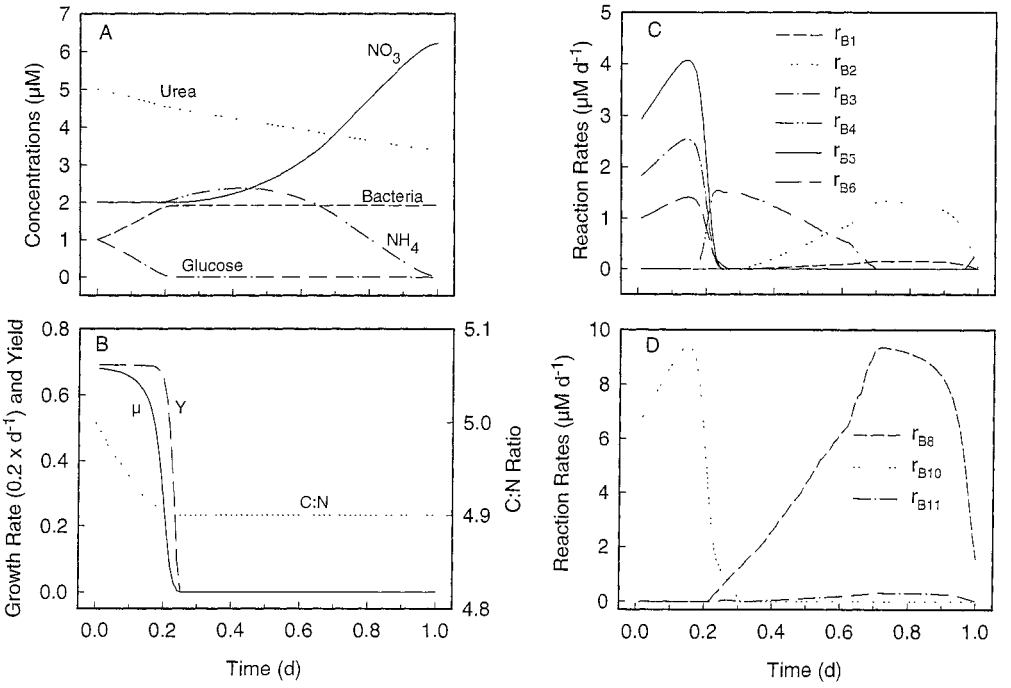

Fig. 7. Simulation 6, with urea and glucose as the DLCN and DLC substrates, respectively. Other conditions as described in the caption of Fig. 2.

Table 8. Substrates used to examine bacterial growth kinetics as a function of degree of reduction (ψ_C) given by Eq. 1 and normalized by C. Free energies of formation (ΔG_f°) are from Thauer et al. (1977) or calculated from Mavrovouniotis (1991).

Substrate	Composition	ΔG_f° (kJ mol^{-1})	ψ_C (per C mol)
Urea	CH_4ON_2	−213	0.0
Oxamate	$C_2H_2O_3N^-$	−514	1.0
Oxalate	$C_2O_4^{2-}$	−674	1.0
Adenine	$C_5H_5N_5$	+321	2.0
Glyoxylate	$C_2HO_3^-$	−474	2.0
Glycine	$C_2H_5O_2N$	−371	3.0
Aspartate	$C_4H_6O_4N_1^-$	−700	3.0
Asparagine	$C_4H_8O_3N_2$	−510	3.0
Glycollate	$C_2H_3O_3^-$	−515	3.0
Arginine	$C_6H_{15}O_2N_4^+$	−240	3.67
Alanine	$C_3H_7O_2N$	−372	4.0
Glucose	$C_6H_{12}O_6$	−917	4.0
Acetate	$C_2H_3O_2^-$	−369	4.0
Lactate	$C_3H_5O_3^-$	−518	4.0
Phenylalanine	$C_9H_{11}O_2N$	−207	4.44
Lysine	$C_6H_{15}O_2N_2^+$	−356	4.67
Valine	$C_5H_{11}O_2N$	−356	4.8
Leucine	$C_6H_{13}O_2N$	−343	5.0
Caproate	$C_6H_{11}O_2^-$	−338	5.33
Palmitate	$C_{16}H_{31}O_2^-$	−267	5.75

concentration was 400 μM and the initial concentration of NH_4^+ was 100 μM. For simulations in which nitrification occurred concurrently with substrate uptake (observed when $\psi_C \leq 1$), we also ran simulations with NO_3^- instead of NH_4^+.

Results show that bacterial yield (Y) exhibits a linear increase with the substrate's degree of reduction per C mole (ψ_C) (Fig. 8A) and is well described ($r^2 = 0.89$) by

$$Y = 0.17\psi_C - 0.038. \quad (17)$$

Bacterial C-specific growth rate (μ d^{-1}) (Fig. 8B) exhibits more scatter, but appears to increase as the square of ψ_C, as given by ($r^2 = 0.86$)

$$\mu = 0.18\psi_C^2. \quad (18)$$

Scatter in the data is due to other factors that affect bacterial growth, such as the substrate's free energy of formation and the variety of elemental combinations that yield the same ψ_C. Substrates with high C:N ratios or that lack N altogether must be augmented with NH_4^+ (or NO_3^-) or C must be dissipated (i.e. oxidized), while N in substrates with low C:N ratios must be remineralized. The C:N ratio of a substrate (ρ_S) is optimal when $\rho_S Y$ equals ρ_B, since neither C nor N need be dissipated (Goldman et al. 1987). Molecular weight also affects bacterial growth kinetics because cellular transport costs (Eq. 5) depend on a substrate's concentration, not on its C, H, O, and N content. Nevertheless, it is clear from the data that bacterial yield and growth rate appear to be largely governed by the substrate's degree of reduction.

Published data on bacterial yield (Fig. 8A, open symbols) are from bioassay studies on specific compounds (Goldman et al. 1987; Heijnen and van Dijken 1992) and whole-system ^{14}C tracer studies (Wright and Shah 1975; Crawford et al. 1974; Hobbie and Crawford 1969; Billen et al. 1980). Although the latter data are not ideal for making comparisons, they do provide good indication of how individual substrates are processed in the presence of a mixture of substrates. What few data do exist seem

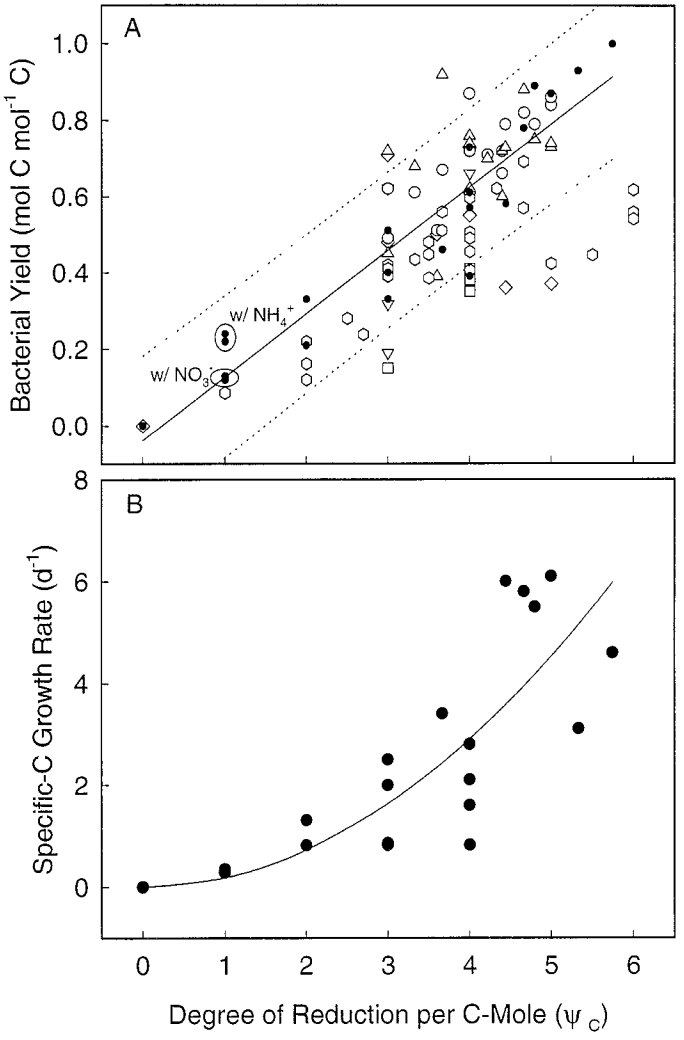

Fig. 8. (A) Bacterial C yield (mol C bacteria/mol C substrate consumed) and (B) specific growth rate (d^{-1}), based on bacterial C, as a function of C-normalized substrate degree of reduction (ψ_C). Filled circles are from simulations of bacterial growth on substrates listed in Table 8, in which the concentration of C-containing substrate was initialized at 400 μM (molecular concentration) and NH_4^+ and/or NO_3^- were initialized at 100 μM. For oxamate and oxalate ($\psi_C = 1$), simulations were run with only NH_4^+ or NO_3^- present (data enclosed by ellipses). Functions (solid lines) were fit to model data only, and the dotted lines specify the 95% prediction intervals. Experimental observations of bacterial yield are shown with open symbols: □—Billen et al. 1980; ○—Crawford et al. 1974; ◇—Goldman et al. 1987; △—Hobbie and Crawford 1969; ▽—Wright and Shah 1975; ○—Heijnen and van Dijken 1992.

to support the relationship between yield and ψ_C for natural systems. This relationship is also supported by work in which a correlation between bacterial yield and the aliphatic content of DOM was observed (Meyer 1994; Sun 1993).

Discussion

We have developed a bioenergetic model that uses basic principles of biochemistry, kinetics, and thermodynamics to help us better understanding the processing of DOM and DIN by bacteria. The model is based on the presumption that competition requires bacteria to maximize growth rate. The overall maximization algorithm is fairly simple and contains relatively few adjustable parameters, but it produces a rich spectrum of results that directly reflect the variety of environmental conditions. Growth characteristics of bacteria have not been directly built into the model as they typically are in Monod-like models (i.e. preference for NH_4^+ over NO_3^-, fixed bacterial C:N ratio, fixed bacterial C yield, fixed maximum specific growth rate, etc.). Instead, general constraints based on first principles are specified for the processing of DOM and DIN into biomass, and the optimization search specifies the set of reaction rates and allocation variables that maximize growth rate for a particular set of conditions. Often, results produced by the model were not anticipated and they required examination to determine why a particular set of reactions was selected as optimum. Such information can often provide insight for interpreting experimental observations. The current model implementation is not intended to predict bacterial growth kinetics with high precision or under all circumstances. Specific pathways regarding the processing of unique substrates are not included; for example, in the model, plastics and hydrocarbons would be processed as easily as lipids. Instead, the model is intended to provide a framework for facilitating the understanding of the basic mechanisms that might control bacterial kinetics.

Substrate limitation of bacterial growth—During the past two decades, microbial ecologists have tried to identify the basic factors that control bacterial growth and yield. Experimental studies have had diverse results and, consequently, there is no agreement at present on the primary controls of bacterial growth. This is not surprising given the variety of approaches and techniques that have been used. Populations have been perturbed with nontracer substrate additions (cf. Suttle et al. 1991), with manipulation of growth medium (cf. Kristiansen et al. 1992), and with long, closed-system incubations (cf. Zweifel et al. 1993) that prevent continuous input of fresh labile DOC, as occurs under in situ conditions (Coffin et al. 1993). In many studies, investigation of the factors that control yield was secondary to another focus, so results have been difficult to interpret. Our bioenergetic model greatly helps in the interpretation of seemingly disparate experimental results.

The many responses that have been observed experimentally for bacterial growth, such as preferential use of dissolved amino acids over glucose and NH_4^+ (Kirchman 1990) or vice versa (Goldman and Dennett 1991), variable dependence on NH_4^+ to meet bacterial N demands (Tupas and Koike 1991; Jørgensen et al. 1993), and N remineralization or immobilization (Kirchman et al. 1989), can be duplicated, at least qualitatively, with our model. Because our modeling results indicate that bacterial response is very sensitive to environmental conditions and bacterial metabolic capabilities, it may be necessary to precisely define the environment and bacterial consortium in order to accurately predict bacterial response. Unless such measurements are made, experiments in which only bulk properties are measured may be difficult to interpret or the interpretations may be over simplified.

To make the model quantitatively match experimental observations, differences in actual metabolic capabilities of the bacteria, such as pathways for glucose but not hydrocarbon utilization, must be accounted for. This can be accomplished by adjusting half-saturation constants (k_i) and placing maximums on allocation variables (a_i) for individual substrates to account for intrinsic metabolic capacities. Differences in actual kinetic parameters are expected because it seems probable that bacterial pathways have evolved control architectures that reflect conditions typically encountered in the natural environment.

It is evident from the model that NH_4^+ is preferentially consumed over NO_3^- (Fig. 3A), a trait that is consistent with observations (Wheeler and Kirchman 1986). The model also switches to preferential uptake of NO_3^- over NH_4^+ when respiration (i.e. oxygen availability) is constrained (data not shown). Indeed, application of our model to investigate bacterial utilization of alternate electron acceptors and donors that occur in anaerobic environments should be profitable.

When uptake kinetics and substrate concentrations are similar, the model indicates that bacteria will preferentially utilize N sources as follows: amino acids, urea, ammonium, nitrate. However, subtle differences in environmental (or experimental) conditions or uptake kinetics owing to changes in bacterial population composition can lead to changes in these preferences. These changes occur because maximum growth rate does not necessarily imply utilization of the most energy-rich compounds. Other constraints, such as substrate consumption per resource investment (i.e. cost) and the complementation of the elemental composition of one substrate with another, play significant roles in the choice of the substrate(s) utilized. Furthermore, changes in environmental conditions, such as substrate availability, can lead to new optimums with only slightly different growth rates, but radically different reaction rates that produce significant alterations in bacterial yield, N processing, and substrate preferences. Consequently, it is difficult and possibly incorrect to generalize results to indicate that growth is limited by C, N, P, temperature, or energy, since it may be that several (or

all) limitations occur simultaneously. For example, how should growth on Phe be described (Figs. 4, 5)? In the first Phe simulation (Fig. 4), bacterial growth during the initial phase (0–0.2 d) appears to be C limited, since DIN concentration is high but is not utilized. However, examination of the reaction rates reveals that excess energy is produced during this phase, which is inconsistent with C-limited growth. In fact, all constraints except energy are active in the initial phase of the Phe simulation. Hence, optimal allocation of resources to maximize growth rate cannot always be rationalized by a single growth limitation. A similar conclusion was reached by Bloom et al. (1985) for resource limitations in plants.

Simple characterization of DOM to predict microbial growth—Analysis of model results from simulations over a range of substrates indicates that bacterial growth rate and yield are strongly dependent on the degree of reduction of the substrate. Experimental data appear to support the relationship, but the data are limited since elemental composition of substrates in most bacterial yield studies was not measured (Bjørnsen 1986; Barillier and Garnier 1993). Indeed, the relationship between yield and degree of reduction has been used in the biotechnology community (Heijnen and van Dijken 1992; Linton and Stephenson 1978), but microbial ecologists do not seem to use this relationship because of the difficulty of measuring the elemental composition of DOM and other environmental variables. However, this may not be an insurmountable problem, as we discuss below.

One of the subtleties associated with the relationship between the C-normalized substrate degree of reduction (ψ_C) and bacterial yield has to do with the concept of refractory material. Although DOM can certainly be made refractory by steric hindrances that protect high-energy compounds from attack by bacterial exoenzymes (Keil and Kirchman 1994), it is also possible that refractory DOM may consist of highly oxidized carbon compounds that are not readily utilized by bacteria owing to their low energy yield. Small compounds that can be readily transported across the bacterial membrane or excreted by phytoplankton should not be considered labile if they are highly oxidized, such as oxalate and perhaps glycollate. Ideally, one should measure the oxidation state of DOM and not just its concentration or even its molecular weight (sensu Benner et al. 1992; Amon and Benner 1994).

Results from the model imply that if the degree of reduction of the substrate can be determined, then bacterial yield and perhaps growth rate can be predicted by Eq. 17 and 18. The most direct approach to measuring ψ_C is to determine the C, H, O, and N composition of DOM with techniques such as those developed by Perdue (1984) and Serkiz and Perdue (1990) and to use Eq. 1. The difficulty with this approach is that it does not distinguish between refractory and labile DOM pools and it requires significant sample preparation. However, it is not necessary to measure the C, H, O, and N composition to determine ψ_C. In the DOM oxidation reaction

$$aCH_\beta O_\gamma N_\delta + bO_2 \rightarrow aCO_2 + cNH_3 + dH_2O \quad (19)$$

it is easy to show from elemental balances that $\psi_C = 4b/a$. Therefore, if DOM is chemically oxidized (either with O_2 or titrated with an oxidizing agent) and there is a quantitative measurement of CO_2 produced and oxidant consumed, then the degree of substrate reduction per C mole can be determined. This approach also measures bulk DOM properties and therefore does not alleviate the problem associated with labile and refractory material; however, the approach may be easier to implement than C, H, O, and N elemental analysis.

Presently, the only methods that distinguish labile and refractory material are bioassays. If a bioassay incubation is conducted with most of the microbial food web intact (i.e. without filtration of eucaryotes), then a substantial fraction of the labile DOM will be oxidized in a stepwise manner through respiration associated with each trophic transfer (i.e. community respiration). So long as the accumulation of POM is small compared to the loss in labile DOM, use of Eq. 19 will provide a good approximation to the overall process, and ψ_C of the labile DOM will approximate $-(4\Delta DO/\Delta DIC)$, where ΔDO and ΔDIC are the changes in dissolved oxygen and dissolved inorganic carbon during the incubation. For bioassays in which significant accumulation of bacterial biomass occurs, Eq. 19 must be augmented as

$$aCH_\beta O_\gamma N_\delta + bO_2 \rightarrow (a - e)CO_2 + cNH_3 + dH_2O + e\,\text{bacteria}. \quad (20)$$

This augmentation accounts for the accumulation of bacteria. The substrate degree of reduction can still be calculated in this case provided that the decrease in DOC ($-\Delta DOC$) is also measured. For this case, ψ_C is given by

$$\psi_C = \frac{e\psi_B - b\psi_{O_2}}{a} = \frac{4.2(\Delta DOC + \Delta DIC) + 4\Delta DO}{\Delta DOC}, \quad (21)$$

where it has been assumed that the accumulation of bacteria, e, is given by the decrease in DOC that is not accounted for in DIC increase. We have also made use of the observed value for the degree of reduction of bacteria (ψ_B) (*see discussion following Eq. 1*). Because the above expressions for ψ_C assume that NH_4^+ is the only DIN participant (consumption of NO_3^- would significantly alter the equations), NH_4^+ should be added as a supplement to these bioassays. Note that this amendment would be for the purposes of characterizing DOM (ψ_C) and not for quantifying the rate or efficiency of degradation, which might be altered.

The relationship shown in Fig. 8A (given by Eq. 17) can be tested; that is, because ψ_C is given by Eq. 21 and bacterial C yield is given by e/a or $(\Delta DOC + \Delta DIC)/\Delta DOC$, new data can be compared to the model output. Presently, the relationships between bacterial yield and growth rate and ψ_C (Eq. 17 and 18 and Fig. 8) are still unproven for mixed bacterial populations in natural environments. Even if these relationships were found to be true, it is not known whether there would be enough variability in ψ_C to make it a good proxy for DOM usability. Nevertheless, the modeling results provide a ra-

tional framework upon which to base experimental approaches.

Theory of ecological thermodynamics—It is uncertain whether bacteria in nature have evolved to maximize growth rate. Indeed, one of the theoretical questions of ecosystems in general that has been debated for decades is whether nature maximizes the ratio of structure (usually measured as biomass, B) to maintenance metabolism (usually measured as respiration, R), $B:R$ (Margalef 1968), or whether it is energy flow itself that is maximized (Odum 1971).

The bioenergetic model is based on the premise that bacteria allocate resources so as to maximize growth rate. This premise is difficult to test because it requires the assessment of metabolic capabilities of the bacterial consortium and the identification of all substrates present in the environment and their concentrations. Although these are areas of active research, it will be some time before precision and accuracy are good enough to rigorously test the model under environmental conditions. However, many of the model results already compare favorably with experimental observations, which would indicate that the premise is operative for at least some subset of conditions. Other theoretical premises could be evaluated by comparing model results based on other optimization goals with experimental observations.

References

AMON, R. M. W., AND R. BENNER. 1994. Rapid cycling of high-molecular-weight dissolved organic matter in the ocean. Nature **369:** 549–552.

ANDERSON, T. R. 1992. Modelling the influence of food C:N ratio, and respiration on growth and nitrogen excretion in the marine zooplankton and bacteria. J. Plankton Res. **14:** 1645–1671.

AZAM, F., AND OTHERS. 1983. The ecological role of water-column microbes in the sea. Mar. Ecol. Prog. Ser. **10:** 257–263.

———, AND E. HODSON. 1977. Size distribution and activity of marine microheterotrophs. Limnol. Oceanogr. **22:** 492–501.

BARILLIER, A., AND J. GARNIER. 1993. Influence of temperature and substrate concentration on bacterial growth yield in seine river water batch cultures. Appl. Environ. Microbiol. **59:** 1678–1682.

BENNER, R., J. D. PAKULSKI, M. MCCARTHY, J. I. HEDGES, AND P. G. HATCHER. 1992. Bulk chemical characteristics of dissolved organic matter in the ocean. Science **255:** 1561–1564.

BILLEN, G., C. JOIRIS, L. MEYER-REIL, AND H. LINDEBOOM. 1990. Role of bacteria in the North Sea ecosystem. Neth. J. Sea Res. **26:** 265–293.

———, ———, J. WIJNANT, AND G. GILLAIN. 1980. Concentration and microbiological utilization of small organic molecules in the Scheldt estuary, the Belgian coastal zone of the North Sea and the English Channel. Estuarine Coastal Mar. Sci. **2:** 279–294.

BJØRNSEN, P. K. 1986. Bacterioplankton growth yield in continuous seawater cultures. Mar. Ecol. Prog. Ser. **30:** 191–196.

BLOOM, A. J., F. S. CHAPIN, AND H. A. MOONEY. 1985. Resource limitation in plants: An economic analogy. Annu. Rev. Ecol. Syst. **16:** 363–392.

BRATBAK, G., AND T. F. THINGSTAD. 1985. Phytoplankton-bacteria interations: An apparent paradox? Analysis of a model system with both competition and commensalism. Mar. Ecol. Prog. Ser. **25:** 23–30.

CARLSSON, P., AND E. GRANELI. 1993. Availability of humic bound nitrogen for coastal phytoplankton. Estuarine Coastal Shelf Sci. **36:** 433–447.

CARON, D. A., J. C. GOLDMAN, AND M. R. DENNETT. 1988. Experimental demonstration of the roles of bacteria and bacterivorous protozoa in plankton nutrient cycles. Hydrobiologia **159:** 27–40.

COFFIN, R. B., J. CONNOLLY, AND P. HARRIS. 1993. Availability of dissolved organic carbon to bacterioplankton examined by oxygen utilization. Mar. Ecol. Prog. Ser. **101:** 9–22.

CRAWFORD, C. C., J. E. HOBBIE, AND K. L. WEBB. 1974. The utilization of dissolved free amino acids by estuarine microorganisms. Ecology **55:** 551–563.

DONGARRA, J. J., AND E. GROSSE. 1987. Distribution of mathematical software via electronic mail. Commun. Assoc. Computing Machines **30:** 403–407.

DUCKLOW, H. W., D. A. PURDIE, P. J. L. WILLIAMS, AND J. M. DAVIES. 1986. Bacterioplankton: A sink for carbon in a coastal marine plankton community. Science **232:** 865–867.

EGLI, T. 1991. On multiple-nutrient-limited growth of microorganisms, with special reference to dual limitation by carbon and nitrogen substrates. Antonie Leeuwenhoek **60:** 225–234.

———, U. LENDENMANN, AND M. SNOZZI. 1993. Kinetics of microbial growth with mixtures of carbon sources. Antonie Leeuwenhoek **63:** 289–298.

FASHAM, M. J. R., H. W. DUCKLOW, AND S. M. MCKELVIE. 1990. A nitrogen-based model of plankton dynamics in the ocean mixed layer. J. Mar. Res. **48:** 591–639.

FOGG, G. E. 1983. The ecological significance of extracellular products of phytoplankton photosynthesis. Bot. Mar. **26:** 3–14.

GOLDMAN, J. C., D. A. CARON, AND M. R. DENNETT. 1987. Regulation of gross growth efficiency and ammonium regeneration in bacteria by substrate C:N ratio. Limnol. Oceanogr. **32:** 1239–1252.

———, AND M. R. DENNETT. 1991. Ammonium regeneration and carbon utilization by marine bacteria grown on mixed substrates. Mar. Biol. **109:** 369–378.

GOTTSCHALK, G. 1986. Bacterial metabolism, 2nd ed. Springer.

HEIJNEN, J. J., AND J. P. VAN DIJKEN. 1992. In search of a thermodynamic description of biomass yields for the chemotrophic growth of microorganisms. Biotechnol. Bioeng. **39:** 833–858.

HOBBIE, J. E., AND C. C. CRAWFORD. 1969. Respiration correction for bacterial uptake of dissolved organic compounds in natural waters. Limnol. Oceanogr. **14:** 528–533.

INGRAHAM, J. L., O. MAALØE, AND F. C. NEIDHARDT. 1983. Growth of the bacterial cell. Sinauer.

JØRGENSEN, N. O. G., N. KROER, R. B. COFFIN, X.-H. YANG, AND C. LEE. 1993. Dissolved free amino acids, combined amino acids, and DNA as sources of carbon and nitrogen to marine bacteria. Mar. Ecol. Prog. Ser. **98:** 135–148.

KEIL, R. G., AND D. L. KIRCHMAN. 1994. Abiotic transformations of labile protein to refractory protein in sea water. Mar. Chem. **45:** 187–196.

KIRCHMAN, D. L. 1990. Limitation of bacterial growth by dissolved organic matter in the subarctic Pacific. Mar. Ecol. Prog. Ser. **62:** 47–54.

———, R. G. KEIL, AND P. A. WHEELER. 1989. The effect of amino acids on ammonium utilization and regeneration by heterotrophic bacteria in the subarctic Pacific. Deep-Sea Res. **36:** 1763–1776.

———, Y. SUZUKI, C. GARSIDE, AND H. W. DUCKLOW. 1991. High turnover rates of dissolved organic carbon during a spring phytoplankton bloom. Nature **352:** 612–614.

KRISTIANSEN, K., H. NIELSEN, B. RIEMANN, AND J. FUHRMAN. 1992. Growth efficiencies of freshwater bacterioplankton. Microb. Ecol. **24:** 145–160.

KROER, N. 1993. Bacterial growth efficiency on natural dissolved organic matter. Limnol. Oceanogr. **38:** 1282–1290.

LASSITER, R. R. 1986. A theoretical basis for modeling element cycling, p. 341–377. *In* T. G. Hallam and S. A. Levin [eds.], Biomathematics: Mathematical ecology. Springer.

LINLEY, E. A. S., AND R. C. NEWELL. 1984. Estimates of bacterial growth yields based on plant detritus. Bull. Mar. Sci. **35:** 409–425.

LINTON, J. D., AND R. J. STEPHENSON. 1978. A preliminary study on growth yields in relation to the carbon and energy content of various organic growth substrates. FEMS (Fed. Eur. Microbiol. Soc.) Microbiol. Lett. **3:** 95–98.

MALCOLM, R. L. 1990. The uniqueness of humic substances in each of soil, steam and marine environments. Anal. Chim. Acta **232:** 19–30.

MARGALEF, R. 1968. Perspectives in ecological theory. Univ. Chicago.

MARLOWE, I. T., R. KAUR, L. J. ROGERS, AND A. J. SMITH. 1989. Extracellular organic production by a picoplankton, *Stichococcus bacillaris*. Phytochemistry **28:** 2993–2997.

MAVROVOUNIOTIS, M. L. 1991. Estimation of standard Gibbs energy changes of biotransformations. J. Biol. Chem. **266:** 14,440–14,445.

MEYER, J. L. 1994. The microbial loop in flowing waters. Microb. Ecol. **28:** 195–199.

MINKEVICH, I. G., AND V. K. EROSHIN. 1973. Productivity and heat generation of fermentation under oxygen limitation. Folia Microbiol. **18:** 376–385.

MOLONEY, C. L., AND J. G. FIELD. 1991. The size-based dynamics of plankton food webs. 1. A simulation model of carbon and nitrogen flows. J. Plankton Res. **13:** 1003–1038.

MOPPER, K., AND OTHERS. 1991. Photochemical degradation of dissolved organic carbon and its impact on the oceanic carbon cycle. Nature **353:** 60–62.

MORAN, M. A., T. LEGOVIC, R. BENNER, AND R. E. HODSON. 1988. Carbon flow from lignocellulose: A simulation analysis of a detritus-based ecosystem. Ecology **69:** 1525–1536.

MOROWITZ, H. J. 1968. Energy flow in biology: biological organization as a problem in thermal physics. Academic.

ODUM, H. T. 1971. Environment, power and society. Wiley.

PACE, M. L., J. E. GLASSER, AND L. R. POMEROY. 1984. A simulation analysis of continental shelf food webs. Mar. Biol. **82:** 47–63.

PERDUE, E. M. 1984. Analytical contraints on the structural features of humic substances. Geochim. Cosmochim. Acta **48:** 1435–1442.

PRESS, W. H., B. P. FLANNERY, S. A. TEUKOLSKY, AND W. T. VETTERLING. 1986. Numberical recipes: The art of scientific computing. Cambridge.

RASHID, M. A. 1985. Geochemistry of marine humic compounds. Springer.

RASTETTER, E. B., AND G. R. SHAVER. 1992. A model of multiple-element limitation for acclimating vegetation. Ecology **73:** 1157–1174.

ROELS, J. A. 1980. Application of macroscopic principles to microbial metabolism. Biotechnol. Bioeng. **22:** 2457–2514.

———. 1983. Energetics and kinetics in biotechnology. Elsevier.

SERKIZ, S. M., AND E. M. PERDUE. 1990. Isolation of dissolved organic matter from the Suwannee River using reverse osmosis. Water Res. **24:** 911–916.

SHERR, E. B., B. F. SHERR, AND L. J. ALBRIGHT. 1987. Bacteria: Link or sink? Science **235:** 88–89.

SIMON, M., AND F. AZAM. 1989. Protein content and protein synthesis rates of planktonic marine bacteria. Mar. Ecol. Prog. Ser. **51:** 201–213.

SMITH, D. C., M. SIMON, A. L. ALLDREDGE, AND F. AZAM. 1992. Intense hydrolytic enzyme activity on marine aggregates and implications for rapid partile dissolution. Nature **359:** 139–142.

STEWARD, G. F., J. WIKNER, W. P. COCHLAN, D. C. SMITH, AND F. AZAM. 1992. Estimation of virus production in the sea: 2. Field results. Mar. Microb. Food Webs **6:** 79–90.

STONE, L. 1990. Phytoplankton-bacteria-protozoa interactions: A qualitative model portraying indirect effects. Mar. Ecol. Prog. Ser. **64:** 137–145.

STOUTHAMER, A. H. 1973. A theoretical study on the amount of ATP required for synthesis of microbial cell material. Antonie Leeuwenhoek **39:** 545–565.

———. 1978. Energy-yielding pathways, p. 389–462. *In* I. C. Gunsalus et al. [eds.], The bacteria: A treatise on structure and function. V. 6. Academic.

SUN, L. 1993. Isolation, characterization, and bioavailability of dissolved organic matter in natural waters. Ph.D. thesis, Georgia Inst. Technol.

SUTTLE, C. A., A. CHAN, AND J. FUHRMAN. 1991. Dissolved free amino acids in the Sargasso Sea: Uptake and respiration rates, turnover times and concentrations. Mar. Ecol. Prog. Ser. **70:** 189–199.

TAYLOR, A. H., AND I. JOINT. 1990. A steady-state analysis of the 'microbial loop' in stratified systems. Mar. Ecol. Prog. Ser. **59:** 1–17.

TAYLOR, G. T., R. ITURRIAGA, AND C. W. SULLIVAN. 1985. Interactions of bactivorous grazers and heterotrophic bacteria with dissolved organic matter. Mar. Ecol. Prog. Ser. **23:** 129–141.

THAUER, R. K., K. JUNGERMANN, AND K. DECKER. 1977. Energy conservation in chemotrophic anaerobic bacteria. Bacteriol. Rev. **41:** 100–180.

TUPAS, L., AND I. KOIKE. 1991. Simultaneous uptake and regeneration of ammonium by mixed assemblages of heterotrophic marine bacteria. Mar. Ecol. Prog. Ser. **70:** 273–282.

TURNER, J. T., AND J. C. ROFF. 1993. Trophic levels and trophospecies in marine plankton: Lessons from the microbial food web. Mar. Microb. Food Webs **7:** 225–248.

WHEELER, P. A., AND D. L. KIRCHMAN. 1986. Utilization of inorganic and ogranic nitrogen by bacteria in marine systems. Limnol. Oceanogr. **31:** 998–1009.

WILLIAMS, P. J. LE B. 1990. The importance of losses during microbial growth: Commentary on the physiology, measurement and ecology of the release of dissolved organic material. Mar. Microb. Food Webs **4:** 175–206.

WOOD, A. M., AND L. M. VAX VALEN. 1990. Paradox lost? On the release of energy-rich compounds by phytoplankton. Mar. Microb. Food Webs **4:** 103–116.

WRIGHT, R. T., AND J. E. HOBBIE. 1966. Use of glucose and acetate by bacteria and algae in aquatic ecosystems. Ecology **47:** 447–464.

———, AND N. M. SHAH. 1975. The trophic role of glycolic acid in coastal seawater. 1. Heterotrophic metabolism in seawater and bacterial cultures. Mar. Biol. **33:** 175–183.

ZHANG, S., G. WEI-BIN, AND V. ITTEKKOT. 1992. Organic matter in large turbid rivers: The Huanghe and its estuary. Mar. Chem. **38:** 53–68.

ZWEIFEL, U. L., B. NORRMAN, AND Å. HAGSTRÖM. 1993. Consumption of dissolved organic carbon by marine bacteria and demand for inorganic nutrients. Mar. Ecol. Prog. Ser. **101:** 23–32.

Submitted: 10 August 1995
Accepted: 20 February 1996
Amended: 20 March 1996